JACS
JOURNAL OF THE AMERICAN CHEMICAL SOCIETY

ARTICLE

pubs.acs.org/JACS

Glutathione Reductase-Catalyzed Cascade of Redox Reactions To Bioactivate Potent Antimalarial 1,4-Naphthoquinones — A New Strategy to Combat Malarial Parasites

Tobias Müller,[†,#] Laure Johann,[†,‡,#] Beate Jannack,[†] Margit Brückner,[†] Don Antoine Lanfranchi,[‡] Holger Bauer,[†] Cecilia Sanchez,[§] Vanessa Yardley,[∥] Christiane Deregnaucourt,[⊥] Joseph Schrével,[⊥] Michael Lanzer,[§] R. Heiner Schirmer,[†] and Elisabeth Davioud-Charvet*[,†,‡]

[†]Biochemie-Zentrum der Universität Heidelberg, Im Neuenheimer Feld 328, D-69120 Heidelberg, Germany

[‡]European School of Chemistry, Polymers and Materials (ECPM), University of Strasbourg, UMR CNRS 7509, 25, rue Becquerel, F-67087 Strasbourg, France

[§]Department of Infectiology, University of Heidelberg, Im Neuenheimer Feld 324, 69120 Heidelberg, Germany

[∥]Department of Infections and Tropical Diseases, London School of Hygiene & Tropical Medicine, Keppel Street, London WC1E 7HT, United Kingdom

[⊥]Muséum National d'Histoire Naturelle, FRE 3206 CNRS, BP 52, 61 rue Buffon, 75231 Paris cedex 05, France

Supporting Information

ABSTRACT: Our work on targeting redox equilibria of malarial parasites propagating in red blood cells has led to the selection of six 1,4-naphthoquinones, which are active at nanomolar concentrations against the human pathogen *Plasmodium falciparum* in culture and against *Plasmodium berghei* in infected mice. With respect to safety, the compounds do not trigger hemolysis or other signs of toxicity in mice. Concerning the antimalarial mode of action, we propose that the lead benzyl naphthoquinones are initially oxidized at the benzylic chain to benzoyl naphthoquinones in a heme-catalyzed reaction within the digestive acidic vesicles of the parasite. The major putative benzoyl metabolites were then found to function as redox cyclers: (i) in their oxidized form, the benzoyl metabolites are reduced by NADPH in glutathione reductase-catalyzed reactions within the cytosols of infected red blood cells; (ii) in their reduced forms, these benzoyl metabolites can convert methemoglobin, the major nutrient of the parasite, to indigestible hemoglobin. Studies on a fluorinated suicide-substrate indicate as well that the glutathione reductase-catalyzed bioactivation of naphthoquinones is essential for the observed antimalarial activity. In conclusion, the antimalarial naphthoquinones are suggested to perturb the major redox equilibria of the targeted infected red blood cells, which might be removed by macrophages. This results in development arrest and death of the malaria parasite at the trophozoite stage.

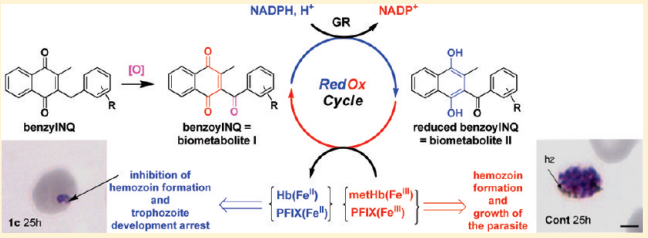

1. INTRODUCTION

Malaria is a major tropical parasitic disease affecting 500 million people worldwide and causing the death of 1−2 million people per year, mostly children in Africa. *Plasmodium* is the causative agent of malaria; the most dangerous species is *P. falciparum*, which is responsible for malaria complications such as cerebral malaria or severe anemia. Multidrug-resistance of *Plasmodium* toward broadly used antimalarial drugs (e.g., chloroquine, sulphadoxine-pyrimethamine) has spread all over the world in the last five decades. Resistance to artemisinin has now emerged.[1] Therefore, new drugs are urgently needed, especially in poor countries. These drugs must be cheap and easy to synthesize, and exhibit mechanism(s) of action that counteract parasite resistance to drugs in use.

The malarial parasite *P. falciparum* digests a large amount of its host cell hemoglobin during the intraerythrocytic cycle as a source of essential nutrients (Figure 1).[2] Hemoglobin digestion takes place in acidic vesicles and in the food vacuole of the parasite;[3a] this leads to the formation of iron(III) ferriprotoporphyrin (FPIX(Fe^{III}) or FPIX−OH(Fe^{III}) or hematin) as a toxic byproduct to the parasite.[3b−e] In the course of this prooxidative process, the parasite is exposed to elevated fluxes of reactive oxygen species.

The parasite evades the toxicity of the released heme by expressing at least two major detoxification pathways, the hemozoin formation in the food vacuole and an efficient thiol network in the cytosol. First, FPIX(Fe^{III}) is polymerized forming crystals of hemozoin or malaria pigment.[4] Second, FPIX(Fe^{III}) is thought to undergo rapid peroxidative decomposition by

Received: February 24, 2011
Published: June 17, 2011

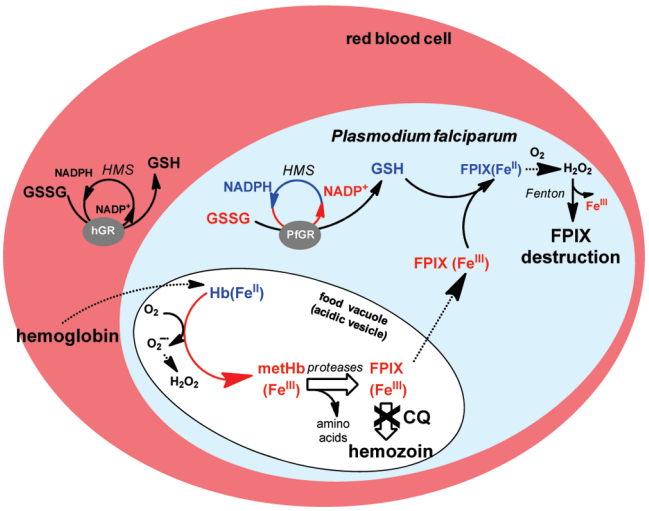

Figure 1. Heme detoxification pathways in the intraerythrocytic cycle of *P. falciparum* and redox homeostasis in *P. falciparum*-infected red blood cell. HMS, hexose monophosphate shunt. CQ, chloroquine is an inhibitor of hemozoin formation (designated by the black X).

reacting with H_2O_2, mainly in the food vacuole, that is, at pH 5.2 where autoxidation of hemoglobin(Fe^{II}) (Hb) takes place.[5] Degradation of heme might also be significant in the cytosol via Fenton reactions, in the presence of glutathione[6] and molecular oxygen following the generation of FPIX(Fe^{II}). A number of antimalarial drugs such as chloroquine (CQ) and related 4-aminoquinolines, quinine, as well as the phenothiazine methylene blue (MB), are known to act as inhibitors of hemozoin formation due to their binding to noncrystalline heme.[3] In sensitive parasites, CQ prevents heme detoxification resulting in free heme accumulation, in the food vacuole and in membranes, which in concert with oxygen species is thought to catalyze oxidation reactions and protein damage causing parasite death.[7] Malarial parasites digest methemoglobin(Fe^{III}) (metHb) faster than Hb(Fe^{II}).[8] Therefore, the reduction of metHb can be used to slow the parasite's metHb digestion rate. Because FPIX(Fe^{II}) is also an inhibitor of heme polymerization,[9] redox-active compounds displaying the ability to reduce FPIX(Fe^{III}) to FPIX-(Fe^{II}) can lead to the decrease of hemozoin formation and increased oxidative stress in infected-red blood cells. Both events would contribute to the arrest of trophozoite development. Thus, agents with redox-cycling activity able to generate Fe^{II} from Fe^{III} states either at the hemoglobin or at the heme levels might act as putative antimalarial agents.

The most important antioxidative system consists of thiols that are regenerated by NADPH-dependent disulfide reductases; these include the glutathione reductases (GR, E.C. 1.8.1.7) from the parasite *P. falciparum* and of human erythrocytes. Both enzymes are targets of antimalarial drugs.[10] These enzymes are essential proteins for the survival of the malarial parasite infecting red blood cells. They maintain the redox equilibrium in the cytosol by catalyzing the physiological reaction, that is, the reduction of glutathione disulfide (GSSG) to its thiol form glutathione (GSH): NADPH + H^+ + GSSG → $NADP^+$ + 2GSH, in particular during the intensive production of reactive oxygen species resulting from hemoglobin digestion.

Different types of inhibitors (reversible, irreversible) were designed in the 1,4-naphthoquinone series[11,12] to evaluate the impact of each inhibition mode on the propagation of the

Scheme 1. Redox-Active 1,4-Naphthoquinones as Subversive Substrates of NADPH-Dependent Disulfide Reductases[a]

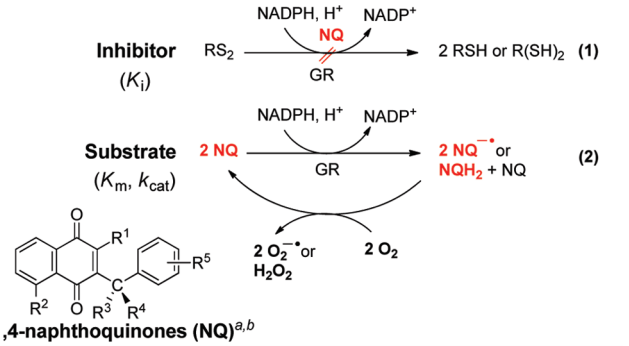

3-benzylmenadione series (R^1 = Me, R^2 = H, CR^3R^4 = CH_2)	**1a-f**
3-benzylplumbagin series (R^1 = Me, R^2 = OH, CR^3R^4 = CH_2)	**2a,2e**
3-benzoylmenadione series (R^1 = Me, R^2 = H, CR^3R^4 = CO)	**3a-f**
3-benzoylplumbagin series (R^1 = Me, R^2 = OH, CR^3R^4 = CO)	**4a**
(±)-3-(α-methylbenzyl)menadione series (R^1 = Me, R^2 = H, CR^3R^4 = CHMe)	**5a,5e**
(±)-3-(phenylhydroxymethyl)menadione (R^1 = Me, R^2 = H, CR^3R^4 = CHOH)	**6a**
3-benzyldifluoromenadione (R^1 = CHF_2, R^2 = H, CR^3R^4 = CH_2)	**7a**
3-benzoyldifluoromenadione (R^1 = CHF_2, R^2 = H, CR^3R^4 = CO)	**8a**

[a] (a) Key structures are shown in Figure 3; (b) R^5 is the series variable.

parasites. They ranged from uncompetitive or catalytic inhibitors (eq 1, Scheme 1),[11a,c] to fluorine-based suicide-substrates,[11b] and their related prodrugs.[12] Considering the different inhibitor types, the most potent antimalarial effects were indeed observed for redox-cyclers acting as subversive substrates (eq 2 and Scheme 1). These compounds are reduced via 1 or 2 electron-(s)-transfer and regenerated in the presence of molecular oxygen, with the concomitant production of superoxide anion radicals.

Starting from an identified lead antimalarial 3-benzylmenadione **1a** (Scheme 1), we report here how we prepared the 3-benzylmenadione analogues **1**, **2**, **5**, **7** (benzylNQ), and **9** (azaNQ) and oriented the investigations to the oxidative metabolism of the potent antimalarial 3-(substituted-benzyl)menadiones **1**, **2** (see general structures in Scheme 1). Because the infected erythrocytes are the target of the lead compound, we hypothesized that the benzylNQ **1a** might be subjected to heme-catalyzed oxidation reactions under oxidative conditions in the acidic vesicles or in the food vacuole as part of the drug bioactivation mechanism (Scheme 2 and Figure 2). On the basis of this hypothesis, we prepared the putative metabolites oxidized in the benzyl position,[13] that is, a menadione (or plumbagin, i.e., 5-hydroxymenadione) substituted by a 3-benzoyl-chain (benzoylNQ) **3**, **4**, and the related "benzhydrol" **6a** (Scheme 1). We also synthesized a series of (±)-3-(α-methylbenzyl)NQ series **5a**,**5e** (Scheme 1) as metabolically resistant derivatives because oxidation might be hampered. To correlate the antimalarial effects of **1a** with the redox system, we envisioned that the GR-reduced naphthoquinone (NQ) might also play a role both in the hemoglobin redox status and the drug bioactivation process (Scheme 2 and Figure 2). Therefore, as a link between the thiol network and the heme metabolism, we showed that the metabolites I, the benzoylNQ, might subsequently be reduced by GR in the cytosols (Scheme 2). Taking into account the putative redox-active behavior of the benzoylNQ metabolites, we then investigated if, in their reduced form, they could convert metHb to Hb in vitro, as MB and menadione do so in vivo.[14] As an expected outcome, we observed

Scheme 2. Putative Redox Cascade Reactions Accounting for the Observed Antimalarial Activity of 3-Benzylmenadione Derivatives

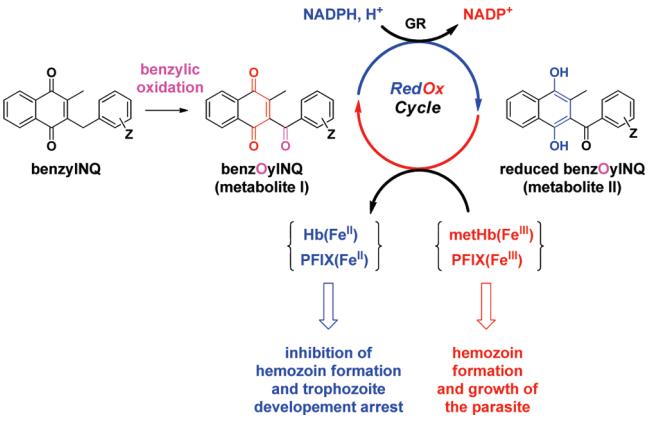

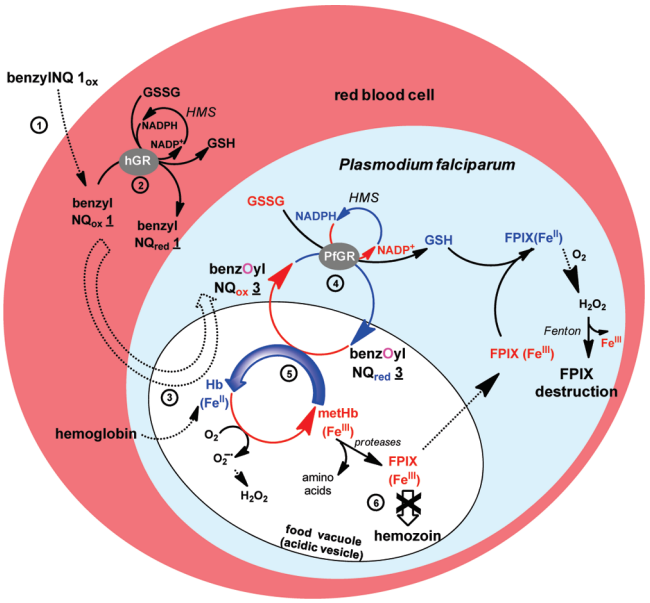

Figure 2. Putative model for lead 1,4-naphthoquinone bioactivation affecting redox homeostasis in *P. falciparum* through a cascade of redox reactions accounting for the observed antimalarial activity of 3-benzylmenadione derivatives. HMS, hexose monophosphate shunt. Blue arrows indicate reduction; red arrows oxidation. Dashed arrows represent uptake processes. The lead benzylNQ are proposed to be taken up by the infected red blood cells (step 1), to be reduced in the cytosol of the human red blood cell by human GR (step 2), and then to be oxidized at the benzylic chain to benzoylNQ in the acidic vesicles or in the food vacuole (step 3) in heme-catalyzed reactions. Subsequently, the benzoylNQ are proposed to be transported into the cytosols and reduced by GR of the human host cell (not shown) or of the parasite (step 4) in a continuous redox cycle. The reduced species of benzoylNQ are assumed to be transported through Fe^{III} complexation into the acidic vesicles where the $benzoylNQ_{red}$ transfer the electrons to oxidants (hematin or metHb, step 5). The final result is an inhibition of hemozoin formation (step 6) and the arrest of trophozoite development as shown in Figure 8. Thus, the antimalarial benzylNQ would act as prodrugs of redox-active principles, being cycled in and out of the acidic vesicles in infected red blood cells, thereby oxidizing major intracellular reductants (NADPH) and subsequently reducing oxidants like hematin or metHb.

Scheme 3. Synthesis of 3-Benzyl and 3-Benzoyl-Substitued Derivatives of Menadione, Plumbagin, Difluoromethylmenadione, and 6-Methylquinoline-5,8-dione[a]

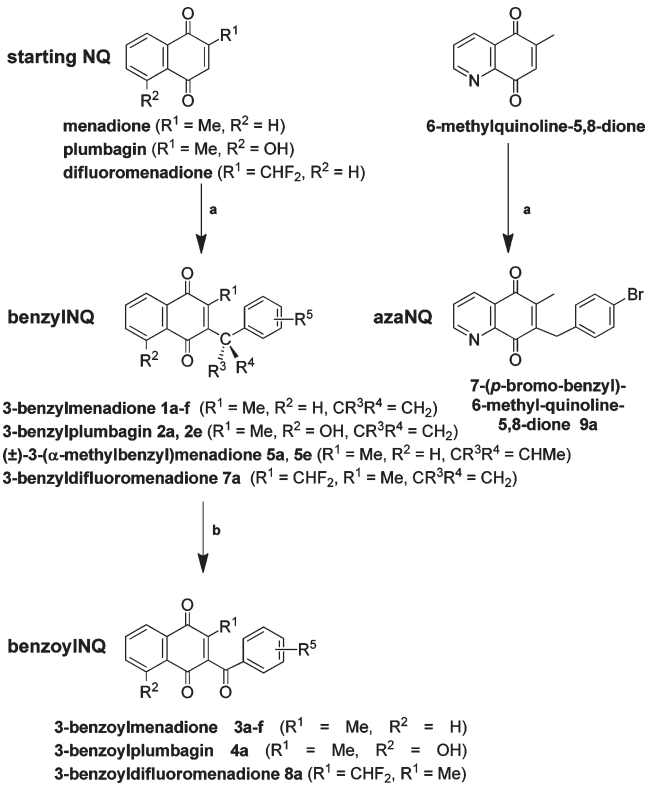

[a] Reaction conditions: (a) phenylacetic acid derivative (2.0 equiv), $AgNO_3$ (0.1 equiv), $(NH_4)_2S_2O_8$ (1.3 equiv), MeCN/water 3/1, 85 °C, 2 h (7−89%); (b) CrO_3 (0.2 equiv), H_5IO_6 (7.0 equiv), MeCN, room temperature, 24 h (33−67%).

an inhibition of hemozoin formation and the arrest of trophozoite development in experiments with synchronized parasites in vitro (step 6 in Figure 2).

Finally, to offer evidence for the concept that the GR-catalyzed bioactivation step is essential for the observed antimalarial activity of the 3-benzylmenadione series, the synthesis of a difluoromethyl analogue (**7a**, Scheme 1) of the lead 3-benzylmenadione **1a** was designed to generate in situ (i.e., in the parasite) the corresponding 3-benzoyl-difluoromenadione metabolite. This compound, the 3-benzoylmenadione **8a**, when synthesized (Scheme 1), was shown to act as a potent suicide-substrate of isolated GRs. Hence, the GR inactivation by the bioreducible alkylating NQ may be correlated with the abolishment of the antimalarial activity of the parent difluorinated benzylNQ **7a**. Our data support the essential role of an active GR within a cascade of redox reactions to bioactivate potent antimalarial 1,4-naphthoquinones. This GR-dependent drug bioactivation process combined with the prodrug effect specifically present in *Plasmodium* via the hematin-catalyzed oxidation reactions represents a new strategy to combat malarial parasites.

2. RESULTS

2.1. Chemistry. We first synthesized a series of menadione, 5-hydroxymenadione (plumbagin), and 5-azamenadione (6-methyl-quinoline-5,8-dione) analogues **1**, **2**, **5**, **7**, and **9** functionalized at

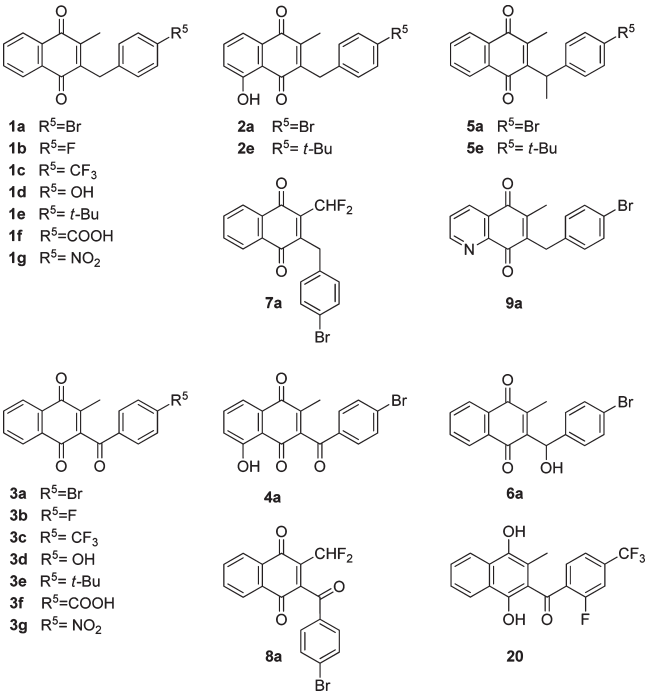

Figure 3. Structures of key 3-substituted benzyl and benzoyl derivatives of menadione, plumbagin, difluoromenadione, and 6-methylquinoline-5,8-dione.

C-3 by a benzyl-chain carrying a broad array of various substituents and tested them for antimalarial activity (Scheme 3, see selected key structures in Figure 3). The silver-catalyzed radical decarboxylation reaction[15] provides a powerful tool for a fast and easy access to 3-substituted-benzyl derivatives of menadione, plumbagin, and 6-methylquinoline-5,8-dione in only one step in moderate to good yields (46−89%, Scheme 3, Table S1 in the Supporting Information) tolerating a wide spectrum of functional groups except for the phenol and the carboxylic acid derivatives (7% for **1d**, and 12% for **1f**). After flash chromatography, all compounds were analytically pure and did not have to be further purified.

The benzoylNQ derivatives **3**, **4** were prepared as putative metabolites of the benzylNQ **1**, **2**. The benzoylNQ were obtained by oxidizing the corresponding benzylic compounds using chromium(VI) oxide and periodic acid as terminal oxidants (Scheme 3).[16] The oxidation reactions from benzyl derivatives **1**, **2** were performed at room temperature for 24 h giving the desired benzoylNQ products **3a**−**f**, **4a**, **8a** in moderate to good yields (33−67%, Scheme 3, Table S1 in the Supporting Information).

The "benzhydrol" **6a** was also prepared as a putative metabolite of **1a** (Scheme 4). Its synthesis followed lithiation of the 2-methyl-3-bromo-1,4-dimethoxy-naphthalene **11** and *p*-bromobenzaldehyde addition to give the benzhydrol intermediate **12**. Oxidation with cerium ammonium nitrate (CAN) afforded the benzhydrol **6a**.

When the benzyl position of the phenylacetic acids was α-alkylated, the yields of the silver-catalyzed decarboxylation were significantly lower (**5a**, **5e**, yields 25−29%, Table S1 in the Supporting Information). The compounds **5a** and **5e** were synthesized via the silver-catalyzed decarboxylation of α-methyl phenylacetic acids, **15a** and **15e**, prepared from phenylacetic methyl esters (Scheme 5). In the case of **5e** bearing a *tert*-butyl

Scheme 4. Synthesis of the (±)-3-(Phenylhydroxymethyl)menadione or "Benzhydrol" 6a[a]

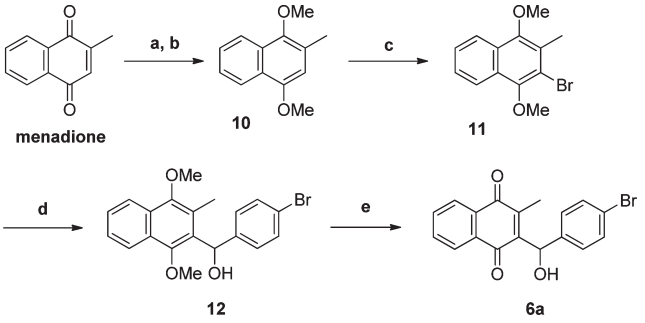

[a] Reaction conditions: (a) 2.5 equiv of $SnCl_2$, HCl, EtOH, room temperature, 0.5 h; (b) 5.0 equiv of KOH, 3.0 equiv of Me_2SO_4, acetone, 60 °C, 2 h (73%); (c) 1.0 equiv of Br_2, CH_2Cl_2, 0 °C, 1 h, then room temperature, 2 h (73%); (d) 1.05 equiv of ^{n}BuLi, THF, −78 °C, 0.5 h, then 1.0 equiv of *p*-bromobenzaldehyde, THF, −78 °C, 10 min, then room temperature, 1 h (73%); (e) 3.0 equiv of CAN, CH_3CN, H_2O, room temperature, 1 h (86%).

Scheme 5. Synthesis of α-Alkylated Carboxylic Acids 15a and 15e and of 3-(α-Methylbenzyl)menadione Derivatives 5a and 5e[a]

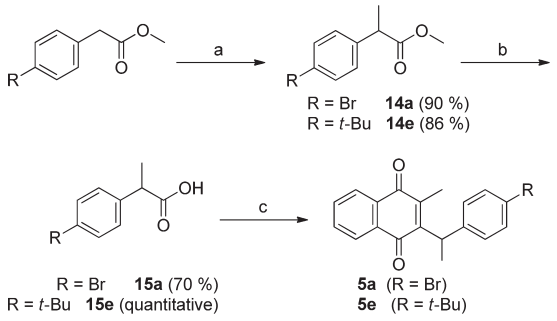

[a] Reaction conditions: (a) lithium diisopropyl amide (LDA), THF, −78 °C, then MeI; (b) EtOH, KOH, H_2O, RT; (c) menadione (1.0 equiv), acid (2.0 equiv), CH_3CN/H_2O (v/v = 3/1), 0.1 equiv of $AgNO_3$, 1.3 equiv of $(NH_4)_2S_2O_8$, 85 °C, 3−4 h.

Scheme 6. Preparation of 2-Difluoromenadione[a]

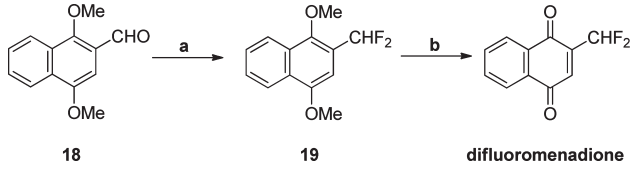

[a] Reaction conditions: (a) 2.0 equiv of DAST, under N_2, room temperature, overnight (90%); (b) 3.0 equiv of CAN, CH_3CN, H_2O, room temperature, 1 h (93%).

group in para-position, the corresponding phenyl acetic acid was synthesized from methyl-*p*-*tert*-butyl-phenylacetate (Scheme 5), which was methylated in α-position to obtain the α-methylacid methyl ester **14e**.

The ester was finally hydrolyzed under basic conditions to obtain the corresponding carboxylic acid **15e** in excellent yield. The same protocol was applied for the synthesis of the

Series	compd	IC_{50} (nM) mean ± SEM (n)
BenzylNQ	**1a**	46 ± 4 (5)
	1b	79 ± 6 (3)
	1c	29 ± 2 (3)
	1d	55 ± 5 (3)
	1e	54 ± 5 (4)
	1f	900 ± 100 (2)
	1g	46 ± 3 (3)
	2a	190
	2e	> 1,000
F-benzyl	**7a**	> 16,000
azaNQ	**9a**	608
Me-benzylNQ	**5a**	306
	5e	218
BenzoylNQ	**3a-f, 4a**	> 1,000
	3g	103
benzhydrol	**6a**	634
F-benzoyl	**8a**	> 1,600
Ref.	**Chloroquine**	110 ± 20 (4)

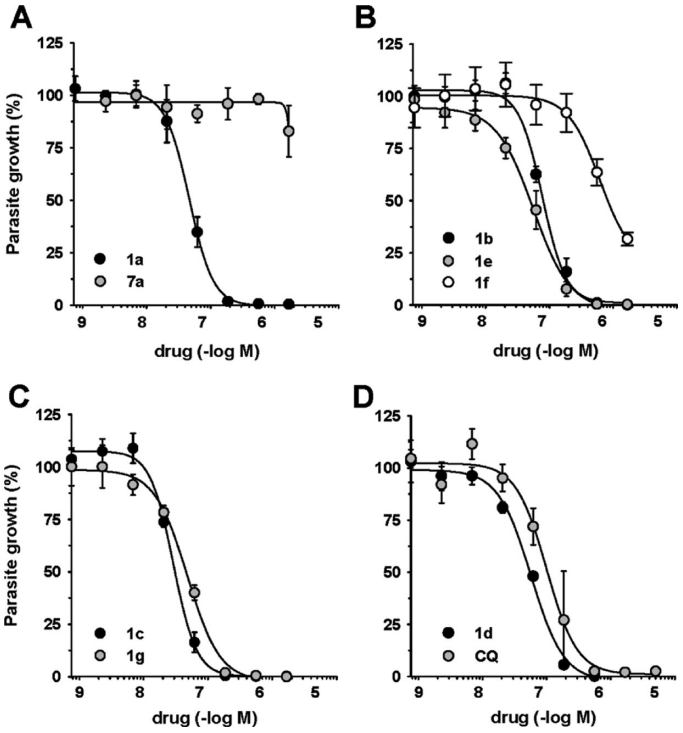

Figure 4. In vitro growth inhibition of malarial parasites (Dd2) by menadione derivatives and dose response curves for a selected number of 3-benzyl representatives. Table: The IC_{50} values were determined using the multidrug resistant *P. falciparum* clone Dd2 in the ^{3}H-hypoxanthine incorporation-based assay.[18,19] Values are the mean ± SEM of (*n*) independent determinations. The IC_{50} value of the antimalarial drug chloroquine is indicated as a reference. Panels A−D: Highly synchronized *P. falciparum* cultures were incubated with increasing concentrations of the compounds indicated, and the percent of parasite growth was determined after 72 h of drug exposure. The data points were fitted using a three-parameter Hill function to calculate the IC_{50} values given in the table. (A) Compounds **1a** (black symbol) and **7a** (gray symbol). (B) Compounds **1b** (black symbol), **1e** (gray symbol), and **1f** (white symbol). (C) Compounds **1c** (black symbol) and **1g** (gray symbol). (D) Compounds **1d** (black symbol) and chloroquine (CQ, gray symbol). The mean ± SEM of at least three independent determinations is shown.

α-methylphenylacetic acid **15a** bearing a bromine atom in para-position, but from ethyl 4-bromophenylacetate as starting material.

The synthesis of the difluoromenadione derivative **7a** was achieved in five steps via the straightforward synthesis of difluoromenadione, prepared by direct fluorination of 1,4-dimethoxy-naphthalene-2-carbaldehyde **18** (Scheme 6). The introduction of the aldehyde function was almost quantitatively achieved (98%) by using 1,4-dimethoxy-naphthalene, dichloromethyl methyl ether, and tin(IV) chloride as reagents.[17] 2-Formyl-1, 4-dimethoxy-naphthalene **18** was treated with diethylaminosulfur trifluoride (DAST) leading to the difluoromethyl-substituted 1,4-dimethoxynaphthalene **19** with an excellent yield (90%). A standard oxidation using CAN as oxidant gave the difluoromenadione in 93% yield (Scheme 6). The benzylation of difluoromenadione was performed through the standard silver-catalyzed decarboxylation reaction of 4-bromo-phenylacetic acid as coupling partner to give **7a** (Scheme 3). Finally, the general procedure for the oxidation of 3-benzyl derivatives using CrO_3/H_5IO_6 was applied to **7a** and led to its benzoyl derivative **8a** in good yield (78%).

2.2. Antimalarial Activities. The library of representative NQ was tested for antimalarial effects using the ^{3}H-hypoxanthine incorporation-based assay (Figure 4).[18,19] Inhibition of the growth of *P. falciparum* by the compounds was evaluated by determining the inhibitor concentration required for killing 50% of the parasite (IC_{50} values). In a screening assay, all compounds were tested against the CQ-resistant *P. falciparum* strain Dd2. Six compounds were revealed with IC_{50} values below 100 nM (table in Figure 4). Key structures are presented in Figure 3. The compounds belong to the 3-benzylmenadione series bearing halide- (**1a**, **1b**, **1c**), hydroxy- (**1d**) functions, nitrogen-based (**1g**), and alkyl-substituent (**1e**). As previously seen, the carboxylic acid function in **1f** is not a favorable parameter for cell bioavalaibility.[11a,12a] In these assays, the standard drug CQ was also tested as reference displaying an IC_{50} value of 110 nM. As compared to the benzyl series, the corresponding benzoyl series displayed lower antimalarial activities with IC_{50} values being greater than 1 μM except in the case of the nitro derivative **3g**.

Concerning the set of key compounds alkylated at the benzyl position, they were designed to study the influence of the "blocked" benzyl position toward the antimalarial activity. The (±)-3-(α-methylbenzyl)NQ **5** series displayed a 3−6-fold decreased antimalarial activity. This suggests an oxidative bioactivation of the parent benzylNQ involving the benzyl chain as part of the mechanism of action. One explanation could be that the benzoyl metabolites need to be generated in the parasite to express their activity. Alternately, contrary to the parent benzylNQ, they might not be recognized by a putative transporter to be internalized by the parasite. This hypothesis remains to be confirmed in the future; we are preparing ^{13}C-enriched benzylNQ representatives to study their metabolism in *P. falciparum*-infected erythrocytes by ^{1}H high resolution magic angle spinning NMR as previously applied for ethionamide pro-drug activation in mycobacteria.[20]

Series	Compd	R^5	IC_{50} (μM) in *P. falciparum* GR assay	IC_{50} (μM) in human GR assay
BenzylNQ	**1a**	Br	> 10[b,c] (nd)[d]	1.0[b] (2.3)[d]
	1b	F	7.8	3.3
	1c	CF_3	> 50	1.6
	1d	OH	8.2	8.6
	1f	COOH	8.0	2.2
	2a	Br	1.0	0.12
F-benzyl	**7a**[e]	Br	13	17
BenzoylNQ	**3a**	Br	1.2	0.3
	3b	F	1.5	1.2
	3c	CF_3	6.3	0.7
	3d	OH	1.8	1.2
	3f	COOH	1.1	0.7
	3g	NO_2	0.8	0.4
	4a	Br	2.5	0.75
F-benzoyl	**8a**[e]	Br	12.0	12.0
Other cpnds	**menadione**[f]	-	42.0	27.5
	difluoro menadione[e]	-	22.8	20
	6a	Br	4.5	1.3
	MB	-	6.4	16.0

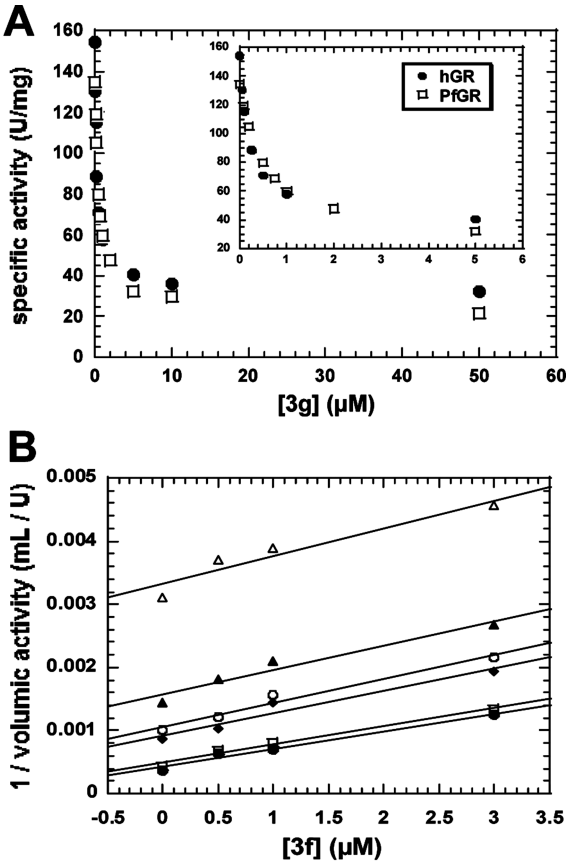

Figure 5. Inhibition of the glutathione reductases from *P. falciparum* and human by 3-benzyl- and 3-benzoyl-substituted derivatives of menadione and dose response curves for the selected 3-benzyl-menadione derivatives **3g** and **3f** as inhibitors of *P. falciparum* and human glutathione reductases under steady-state conditions. Table: (a) The values were determined at pH 6.9 and 25 °C in the presence of 1 mM GSSG; (b) in the presence of 5% dimethyl sulfoxide (DMSO); (c) reprecipitation of the compound in the cuvette prevented IC_{50} determination; (d) in the presence of 1% DMSO; (e) concomitant aggregation of the enzyme occurred; (f) data from ref 11b. nd: not determined. Panel A: Dose response curves for the selected 3-benzylmenadione **3g** as inhibitor of *P. falciparum* (□) and human (■) glutathione reductases in the presence of 1 mM GSSG as disulfide substrate and 100 μM NADPH. Panel B: Dixon plot showing inhibition of *P. falciparum* GR-catalyzed GSSG reduction at a fixed NADPH concentration (100 μM) in the presence of GSSG as variable substrate (20 (Δ)−40 (▲)−60 (○)−100 (♦)−400 (□)−1000 (●) μM) and increasing **3f** concentration (0−0.5−1−3 μM). 1% final DMSO was present in experiments.

2.3. Glutathione Reductase Inhibition Studies. *Determination of IC_{50} Values.* As a consequence of their potential substrate competence, the 3-benzyl- and 3-benzoylmenadione analogues were first tested as inhibitors of both GRs in the standard 1 mM GSSG reduction assay (table in Figure 5). 2-Methyl-1,4-naphthoquinone (menadione) was used as reference, displaying IC_{50} values of 42.0 and 27.5 μM for *P. falciparum* GR and human GR respectively. All compounds (Figure 5) displayed higher GR inhibition potencies than did the unsubstituted menadione. In addition, the 3-benzoylmenadiones **3**, **4** behaved as the most potent GSSG reductase inhibitors described so far, with IC_{50} values up to 10-fold lower than for the 3-benzyl analogues **1**, **2** (Figure 5A). In general, all compounds showed a 1.25−9-fold stronger inhibition for human GR than for *P. falciparum* GR, assuming a stronger interaction with human GR. Compound **3f** was then selected for detailed inhibition studies to determine the inhibition type and constants in *P. falciparum* GR assays.

Inhibition Type of P. falciparum and Human Glutathione Reductase under Steady State. To investigate the type of *P. falciparum* GR inhibition, kinetics were performed at various concentrations of both GSSG and potent inhibitor **3f**, in the presence of a saturating NADPH level. The data were fitted to the appropriate equation with Kaleidagraph using a computerized least-squares regression program. With GSSG (20−1000 μM) as variable substrate and NADPH at a constant concentration of 100 μM, the K_m value of GSSG in the absence of inhibitor was found to be 144.4 ± 15.7 μM. The inhibition of *P. falciparum* GR by **3f** (0−3 μM) was found uncompetitive with respect to GSSG. The K_i value for **3f** was determined as 1.0 ± 0.06 μM from the secondary plot expressing $1 + [I]/K_i$ as a linear function of inhibitor concentration. The uncompetitive type of inhibition of *P. falciparum* GR by **3f** was deduced from Cornish−Bowden, Lineweaver−Burk, and Dixon (Figure 5B) plots. In the human GR assay also assuming uncompetitive inhibition, the K_i value for **3f** was determined as 0.64 ± 0.02 μM with respect to GSSG.

Glutathione Reductase-Catalyzed Naphthoquinone Reductase Activity. The ability of *P. falciparum* GR to reduce the 1,4-naphthoquinones was studied in vitro by following the oxidation of NADPH in the presence of various 3-benzyl- and 3-benzoyl menadione derivatives and was compared to menadione itself as reference (Table 1). The NQ reductase activity of *P. falciparum* GR was compared to the intrinsic NADPH oxidation activity of the enzyme in the absence of the NQ. The catalytic parameters of menadione against *P. falciparum* GR were shown[11a] to be

Table 1. *Plasmodium falciparum* Glutathione Reductase-Catalyzed Naphthoquinone Reduction[a]

			naphthoquinone reductase activity of *Pf*GR[a]		
series	compd	R^5	K_m (μM)	k_{cat} (min^{-1})	k_{cat}/K_m ($mM^{-1}\ s^{-1}$)
benzyl	**1a**	Br	nd[b]	nd[b]	nd[b]
	1b	F	26	2.53	1.62
	1d	OH	67	2.54	0.64
benzoyl	**3a**	Br	6.1	2.31	6.31
	3b	F	56.1	16.7	4.96
	3c	CF_3	42.4	3.36	1.32
	3d	OH	84.2	26.6	5.26
	3g	NO_2	18	8.38	7.76
	3f	COOH	1325	111.6	1.4
	4a	Br	3.07	2.3	12.5
benzhydrol	**6a**	Br	8.5	2.17	4.25
ref	menadione		82.2	9.6	1.99[c]
	MB		42.2	34.8	13.7

[a] For GSSG as a substrate of *Pf*GR: $K_m = 83\ \mu M$, $k_{cat} = 9900\ min^{-1} = 165\ s^{-1}$, $k_{cat}/K_m = 1988\ mM^{-1}\ s^{-1}$. [b] Precipitation of the compound was observed above 10 μM; at 10 μM there is no inhibition. [c] From ref 11a.

82.2 μM and 9.6 min^{-1} for K_m and k_{cat}, respectively, leading to a catalytic efficiency k_{cat}/K_m of 1.99 $mM^{-1}\ s^{-1}$ (Table 1).

As compared to menadione as reference, the tested compounds **1a**−**d**, **3a**-**g**, and **4a** bearing a various set of substituents showed low K_m values ranging from 6.1 μM (**3a**) to 56.1 μM (**3b**), indicating a tighter binding to the enzyme *Pf*GR, while **3d** with a K_m value of 84.2 μM showed similar apparent Michaelis−Menten constant. From the catalytic efficiencies, expressed as k_{cat}/K_m values, **3a**, **3b**, **3d**, **3g**, **6a**, and **4a** behaved as very effective substrates of *Pf*GR, among the most efficient subversive substrates of *P. falciparum* GR described so far. In contrast, when different concentrations of **3f** were used, catalytic constants expressed as a k_{cat} of 1.86 s^{-1} and a K_m value of 1324.6 μM were determined assuming Michaelis−Menten kinetics. The high K_m value for the carboxylic acid function in the napthtoquinone reductase activity was previously observed for analogues.[11a] Compounds with two redox active moieties like **3g** (with a nitrophenyl group) showed a 3.9-fold increased catalytic efficiency when compared to menadione. Also, an increased oxidant character, expressed with the plumbagin derivative **4a**, led to 6.3-fold higher catalytic efficiency than that of menadione and a value similar to that of MB.

2.4. Abolishment of the Antimalarial Activity by Glutathione Reductase Inactivation. Interestingly, the 3-benzyldifluoromenadione **7a**, an analogue of the active lead **1a**, was found to have almost no effect in antimalarial screening assays ($IC_{50} > 16\ \mu M$, Figure 4). This abolishment of the antimalarial activity suggested that the presence of the fluorine atoms at the methyl group inhibited the drug metabolism in the *Plasmodium*-infected erythrocytes. Because its benzoyl metabolite was expected to be generated in the parasite in situ, the 3-benzoyldifluoromenadione **8a**, analogue of the active lead **3a**, was synthesized and tested as a suicide-substrate of both GRs.

As shown earlier with monofluoromenadione derivatives[11b] (Scheme 7), it has been confirmed that reduction by NADPH is a prerequisite for irreversible GR inhibition by the suicide-substrate, 6-[2′-(3′-fluoromethyl)-1′,4′-naphthoquinolyl]hexanoic acid (fluoroM_5), and time-dependent inactivation resulted in alkylation of human GR at Cys58 of the redox active dithiol.[11b]

Scheme 7. Time-Dependent Inactivation of Human Glutathione Reductase by Monofluoromenadione Derivatives

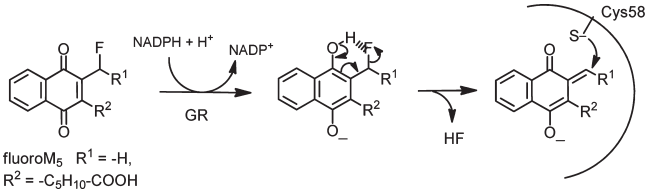

Noteworthy is the previous observation made with these monofluorine-based suicide-substrates of glutathione reductases: irreversible GR inhibition did not lead to increased antimalarial effects but instead to increased toxicity toward human cells.

The presence of one, two, or three fluorine atoms has an influence on the oxidant character of the parent menadione core. The electrochemical properties of the fluoromethyl compounds were investigated by cyclic voltammetry under the conditions previously described.[11b] Both with the trifluoromenadione ($E^\circ_1 = -0.308$ V/standard calomel electrode (SCE)) and the difluoromenadione ($E^\circ_1 = -0.385$ V/SCE), one-electron reduction occurred at less negative values than with menadione used as reference ($E^\circ_1 = -0.650$ V/SCE). These values make these two fluoro analogues of menadione strong oxidants and potential effective substrates of both glutathione reductases. In contrast to menadione showing redox reactions kinetically reversible in the cyclic voltammogram (data not shown), the formation of the quinone methide species followed by polymerization in the case of the difluoromenadione might be responsible for the non reversibility of the electron transfer reactions. These observations are in agreement with earlier literature,[11b,21] rendering the difluoromenadione more prone to act as a suicide-substrate.

When following NADPH consumption at 340 nm in the enzymic assays, the difluoromenadione was reduced by *P. falciparum* GR with a catalytic efficiency k_{cat}/K_m of 155.9 $mM^{-1}\ s^{-1}$, a value 12.7-fold lower than that determined for the physiological substrate GSSG but 82-fold higher than that determined for menadione (Table 2).

Table 2. Kinetic Parameters of Human and *P. falciparum* Glutathione Reductases with Fluoromethyl Analogues of Menadione as Substrates

compd	GR species	K_m (μM)	k_{cat} (s^{-1})	k_{cat}/K_m (mM^{-1} s^{-1})
menadione	*h*	31.2	0.16	5.1
menadione	*Pf*	87.4	0.17	1.9
difluoro menadione	*h*	66.2	6.7	101.4
difluoro menadione	*Pf*	82.1	12.8	155.9

Table 3. Selected Kinetic Parameters of Human Glutathione Reductase Inactivation by Fluoro Menadione Analogues

compd	$t_{1/2}$ (min)	K_I (μM)	k_i (min^{-1})	k_i/K_I (mM^{-1} s^{-1})
difluoro menadione	0.1	66.2	7.0	1.8
7a	27.7	16.8	0.025	0.025
8a	0.08	8.9	9.0	16.9

With the difluoromenadione, **7a** (benzylNQ) and **8a** (benzoylNQ), the two difluoromethyl analogues of the 3-benzyl- and the 3-benzoyl-menadione derivatives **1a** and **3a**, respectively, time-dependent inhibition of the GRs from man and *P. falciparum* was studied using the 1 mM GSSG reduction assay to evaluate the residual activity of reacted enzymes. Upon incubation with NADPH and the suicide-substrates, inactivation of human GR by the three compounds followed pseudofirst-order reaction kinetics. The experimental data allowed the application of the derivation by Kitz and Wilson[22] for irreversible inactivation. A semilogarithmic plot of the fraction of noninhibited enzyme activity $\ln(v_i/v_0)$ versus incubation time yielded straight lines with increasing slopes at short time periods, equivalent to the apparent rate constant of irreversible inhibition (k_{obs}). The secondary plot expressing k_{obs} as a function of inhibitor concentration followed eq 3:

$$k_{obs} = \frac{k_i[I]}{K_I + [I]} \quad (3)$$

where K_I is the dissociation constant of the inhibitor−enzyme complex and k_i is the first-order rate constant for irreversible inactivation, respectively. The k_{obs} data versus [**8a**] (or [**7a**] or [difluoromenadione]) were fitted to eq 3, which resulted in the hyperbolic curve and the determination of the dissociation constant for the **8a**−, the **7a**−, or the difluoromenadione−GR complexes and the first-order rate constant for irreversible inactivation, respectively, as $K_I = 8.9 \pm 4.0$ μM and k_i as 9.0 ± 1.8 min^{-1} for **8a** (versus 16.8 μM and 0.025 min^{-1} for **7a** and 66.2 μM and 7.0 min^{-1} for the difluoromenadione), allowing estimation of a second-order rate constant k_i/K_I as 16.9 mM^{-1} s^{-1} for **8a** versus 0.025 for **7a** and 1.8 mM^{-1} s^{-1} for difluoromenadione (Table 3). The resulting half-times ($t_{1/2}$) of inactivation of the human GR were determined as 0.1 min and below 0.1 min for the difluoromenadione and **8a**, respectively, versus 27.7 min for **7a** (Table 3).

Interestingly, the IC_{50} values of the difluoro-naphthoquinones (difluoromenadione, **7a**, **8a**) determined in GR-catalyzed GSSG reduction assays under steady conditions were found to be 1 order of magnitude higher than the values for the benzoylNQ series, **3a**−**g** (see Table in Figure 5). The dose response curves for the 3-benzoyl-menadione **3a** and -difluoro-menadione **8a** derivatives in GSSG reduction assays in the presence of the human GR are shown in Figure 6. They are thought to result from two events: NADPH consumption due to GSSG reduction catalyzed by free homodimeric human GR in solution and polymerization of the difluoro quinone methide generated from the difluoromenadione derivative in the presence of the reduced enzyme. The high reactivity of the difluoro quinone methide intermediate is likely to act as a cross-linking reagent, by analogy to acrolein and its difluoro analogue in polyacroleins formation (see below).[23]

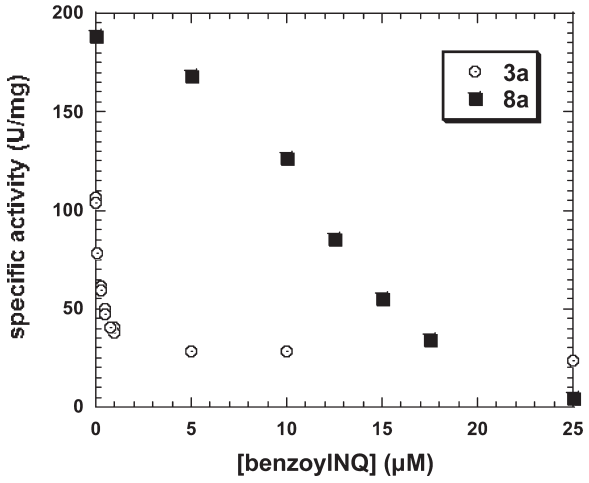

Figure 6. Dose response curves for the 3-benzoyl-menadione **3a** and -difluoromenadione **8a** derivatives as human glutathione reductase inhibitors under steady-state conditions. From the dose response curves recorded at pH 6.9 and 25 °C in the presence of 1 mM GSSG as disulfide substrate, 100 μM NADPH, and 1% DMSO, the IC_{50} values for the selected 3-benzoylmenadione derivatives **3a** (□) and **8a** (■) were determined as 0.3 and 12 μM, respectively.

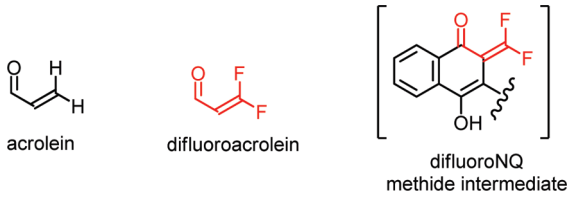

The results are consistent with our concept of an irreversible mechanism-based inhibition by 3-benzoyl-difluoromenadione derivatives. In additional kinetic experiments (data not shown), we observed that *Plasmodium* GR was also quickly inactivated upon incubation of the enzymes with NADPH and **8a**. The first-order rate constant k_i for irreversible inactivation could not be determined because of the concomitant inactivation of the parasitic enzyme by NADPH itself in open air.[11b] Thus, the irreversible GR inactivation by a fluorine-based suicide-substrate of both GRs designed to be generated from **7a** in the parasites, the benzoylNQ **8a**, was accompanied by a complete loss of the antimalarial activity of both the 3-benzylmenadione **7a** and the 3-benzoylmenadione **8a**. These results suggest the essential requirement of an active GR (either the human or the parasitic enzyme, or both) in the drug bioactivation of the antimalarial lead benzylNQ **1a**.

2.5. Methemoglobin Reduction in the Presence of the Redox-Active BenzoylNQ. To evaluate the reduction of metHb to Hb, we set up an assay using the benzoylNQ, metHb(Fe^{III}), and the glutathione reductase/NADPH-based system to regenerate

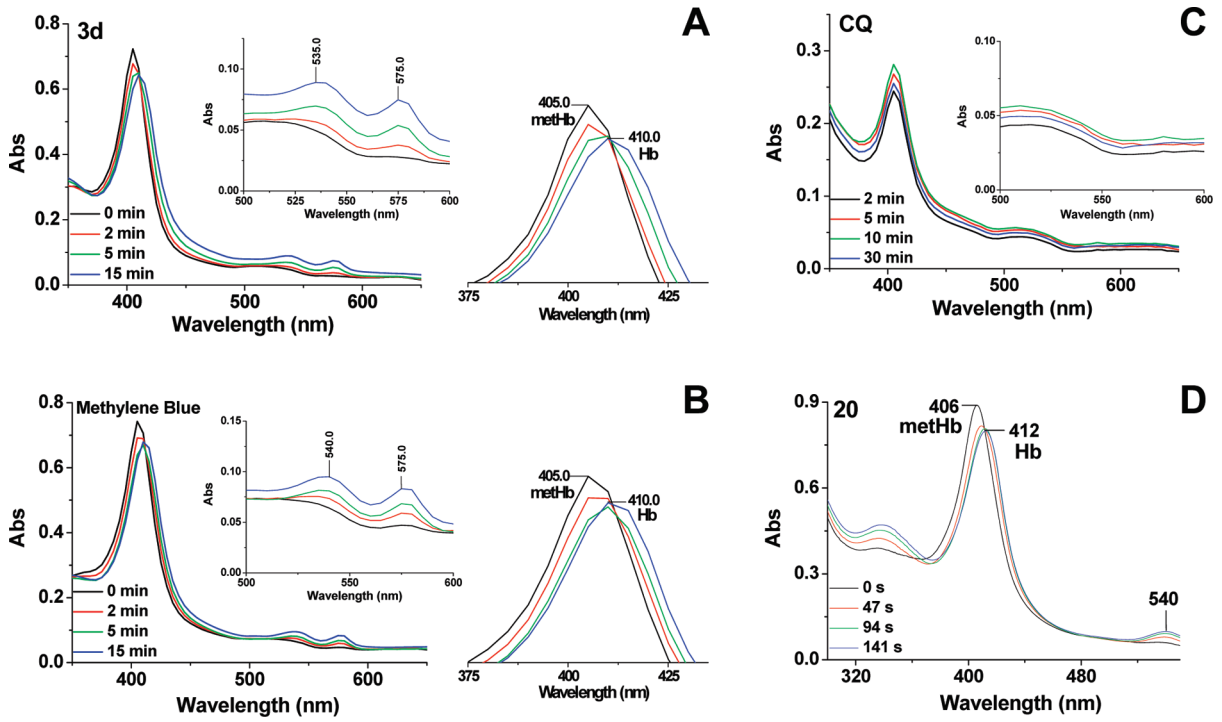

Figure 7. Methemoglobin reduction by the glutathione reductase/NADPH-reduced redox-active agents, benzoylNQ **3d** or methylene blue, or through the direct reaction with the 3-benzoyl-dihydronaphthoquinone **20**. UV−vis absorption spectra evidencing the reduction of metHb(Fe^{III}) to Hb(Fe^{II}) in the coupled assay based on the human GR/NADPH system in the presence of the subversive substrate benzoylNQ **3d**, or **MB**, and the direct reduction of metHb(Fe^{III}) to Hb(Fe^{II}) by the dihydrobenzoylNQ **20**. Panel A: The reaction of 200 μM **3d** in the presence of 100 μM metHb, 400 μM NADPH, 1 μmol human GR, final [DMSO] 1%, at 37 °C caused a shift in the λ_{max} of metHb (from 405 to 410 nm). Spectra were measured at different times over a 15 min period following addition of 20 μL of the reaction mixture to a 1 mL cuvette containing GR buffer, pH 6.9. Panel B: Methylene blue was used as a positive control under the same conditions; a clear shift of λ_{max} of metHb was observed from 405 to 410 nm. Panel C: CQ was used as a negative control. As expected, no shift was observed in the presence of CQ. The conditions used in the reaction mixture were 50 μM metHb, 100 μM CQ, 200 μM NADPH, and 1.06 μmol hGR, final [DMSO] 1%, 37 °C. Panel D: The conditions used in the reaction mixture were 2 μM metHb, 40 μM dihydrobenzoylNQ **20**, final [DMSO] 2% in GR buffer, pH 6.9, at 37.5 °C. The reaction was started directly in the cuvette, and UV−vis absorption spectra were recorded as a function of time.

the hydronaphthoquinone continuously. The UV spectrum of metHb between 300 and 700 nm is characterized by a maximal absorbance at 405 nm, and a broad band centered at 630 nm. Figure 7A displays reduction of metHb in the presence of the benzoylNQ **3d**, characterized by a k_{cat}/K_m of 5.26 mM^{-1} s^{-1}, continuously reduced by the human GR/NADPH-based system. Upon metHb reduction, the spectrum of Hb(Fe^{II}) showed a shift of the maximal absorbance from 405 to 410 nm and two weak bands at 536 and 576 nm (Figure 7A). MB with a k_{cat}/K_m value of 13.7 mM^{-1} s^{-1} was used as a positive control of this effect (Figure 7B). In the coupled assay, the shift of the maximal absorbance from 405 to 410 nm is already visible at 20 μM MB, or at 100 μM menadione (data not shown), or at 50 μM benzoylNQ **3d**. As expected, no band shift was observed in the presence of CQ instead of the benzoylNQ nor in the presence of MB (Figure 7C).

To confirm the electron transfer from the reduced 3-benzyl-naphthoquinones to MetHb(Fe^{III}), the direct reduction of methemoglobin MetHb(Fe^{III}) by a 3-benzoyl-dihydronaphthoquinone derivative was evaluated (in the absence of the GR/NADPH system). Because the 3-benzoyl-dihydronaphthoquinone derivatives are quite unstable in open air and very prone to be quickly reoxidized into naphthoquinones, a "stabilized" 3-benzoyl-dihydronaphthoquinone derivative **20** (Figure 3) was prepared. This compound possesses a fluorine atom in ortho position to the methanone group, which likely stabilizes the β-hydroxyketone bridge via hydrogen bonds. In that case, a complete reduction of metHb(Fe^{III}) to Hb(Fe^{II}) was observed in 2 min in the absence of the regenerating GR/NADPH system (Figure 7D).

2.6. Cytotoxic Activities against Human Cells in Vitro. Noteworthy is the absence of hemolysis of infected and non-infected red blood cells, at the highest micromolar drug concentrations tested (30 μM). In addition, all compounds were tested for cytotoxicity against two human cell lines, the human buccal carcinoma cell line cell (KB) and the human lung MRC-5 fibroblasts, by using the Alamar blue assay (Table S2 in the Supporting Information). Most of the 1,4-naphthoquinone derivatives exhibited a low cytotoxicity profile against both human KB and MRC-5 cell lines as evidenced by the high IC_{50} values above 32 μM. The toxicity of the two derivatives, 3-benzyl-difluoromenadione **7a** and the oxidant azamenadione **9a**, probably stems from the higher lipophilicity due to the presence of fluorine atoms and/or from their high oxidant character,[11c] respectively. Furthermore, when tested in Ames test, the lead benzylNQ **1c**, up to 100 μM, did not induce mutagenicity using three strains of *Salmonella thyphimurium* TA98, TA100, and TA1535 (the complete data of the genotoxicity study will be published elsewhere).

2.7. Antimalarial Activities in *Plasmodium berghei*-Infected Mice. Five of the most active compounds (**1a**, **1c**, **1d**, **1e**, **1g**),

dx.doi.org/10.1021/ja201729z |*J. Am. Chem. Soc.* 2011, 133, 11557–11571

Table 4. Reduction of Parasitemia in CD1Mice Infected with *Plasmodium berghei* Strain ANKA[a]

compd	dose (mg/kg × 4)	reduction ip[b] (%)	reduction po[b] (%)	*p*-value[c]
untreated control		0	0	
CQ[a]	10	94.9	98.8	0.0079
1a	30		0	ns
1a	50	35.6	0.8	0.0079
1c	30	20.7		ns
1d	30	28.4		ns
1g	30	42.4	10.4	ns
1e	30	43.4	34.9	0.0079

[a] In this assay, at 1.0, 3.0, and 10.0 mg/kg po, chloroquine displayed a reduction of the parasitemia of 2.5%, 16.6%, and 94.9%, respectively. [b] ip and po stand for intraperitoneal and oral administration, respectively. [c] Calculated in the two-tailed Mann−Whitney U test on the differences of treated versus untreated mice. ns means non significant.

which had successfully passed all studies with parasites in cultures, were subsequently tested for their antimalarial action in vivo using the murine CD1 malaria model infected by the CQ-susceptible ANKA strain of *P. berghei*. Results of in vivo screens for the five compounds conducted according to the Peters's 4-day test are given in Table 4. For comparative purposes, data for CQ and the five derivatives upon intraperitoneal administration (ip) acquired in the same screens were included. The untreated control group showed no decrease in parasitemia after ip or oral (po) administration. CQ as reference was applied at a dose of 10 mg/kg ip and po; the parasitemia decreased by 94.9% and by 98.8%, respectively. Compounds **1a**, **1c**, **1d**, **1e**, and **1g** showed significant activity following a 4-day treatment.

Compound **1a** was administered at 50 and 30 mg/kg per day. There was no significant inhibition when the compound was given orally, but there was a significant effect, 35.6% inhibition (p-value = 0.0079), when given intraperitoneally at 50 mg/kg. The two most active drugs **1e** (*t*-Bu derivative) and **1g** (nitro derivative) caused 43.4% and 42.4% reduction of parasitemia, using a daily dose of 30 mg/kg ip, respectively. At this dose level, **1c** (CF_3 derivative) and **1d** (phenol) displayed a 20.7−28.4% decrease of parasitemia, suggesting a poor bioavailability or a high rate of drug clearance due to rapid elimination in the host. Upon oral administration of the two most active drugs **1e** and **1g** at 30 mg/kg per day, the parasitemia was reduced to 34.9% and 10.4%, respectively. So far, the efficiency of **1a** has been improved by preparing a metabolically resistant analogue by introduction of a *t*-Bu group in the critical position for biooxidation.[24] The data in Table 4 support an oxidative metabolism in vivo (see **1a** data versus **1e** data); that is, **1e** is equally active by ip (43.4%) and po (34.9%) administration, while this does not apply for **1a**. More chemistry is required to improve the efficiency of the **1a** series in vivo.

2.8. Inhibition of the Development of *P. falciparum* Trophozoites by Compound 1c. The intraerythrocytic cycle of *P. falciparum* begins when the infective form of the parasite invades an erythrocyte, and it ends 48 h later when multiple new infective parasites escape from the host cell. In the meantime, *Plasmodium* has developed through ring (0−20 h postinvasion (p.i.)), trophozoite (20−36 h p.i.), and schizont (36−48 h p.i.) stages. Because trophozoite is the most active stage at digesting host cell hemoglobin, we assessed whether compound **1c** might inhibit trophozoite development. As determined from dose−response assays, compound

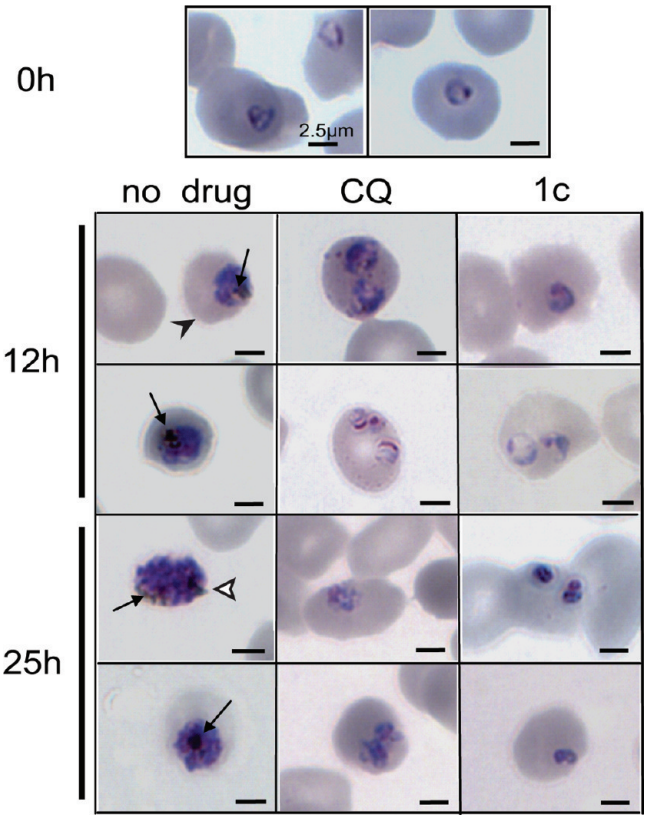

Figure 8. Compound **1c**-induced inhibition of *P. falciparum* trophozoite development. Optical examination of compound **1c**-induced inhibition of *P. falciparum* trophozoites was performed microscopically. Synchronized parasites at the trophozoite stage of the intraerythrocytic cycle (i.e., 16−21 h posterythrocyte invasion) were grown either in normal culture medium (no drug) or in culture medium supplemented with 5 μM chloroquine (CQ) or 5 μM compound **1c**. Diff Quick-stained smears were prepared from aliquots of the cultures at different time points. Details from smears at 0 h (16−21 h-old parasites), 12 h (28−33 h-old parasites), and 25 h (41−46 h-old parasites) of incubation are presented. Hemozoin in the parasite food vacuole is indicated by an arrow. Black arrowhead: erythrocyte. Note the multinucleated parasite (empty arrowhead) after 25 h in normal culture (no drug). Scale bar: 2.5 μm. Photographs: Metamorph software, Power Point/Illustrator software.

1c inhibits FcB1 trophozoite growth with a 0.90 μM IC_{50} value and an estimated 5 μM $IC_{100\ min}$. Chloroquine IC_{50} and IC_{100} values on FcB1 trophozoites were 0.25 and 2 μM, respectively. As shown in Figure 8, maturation of young trophozoites was dramatically altered in the presence of 5 μM compound **1c** (column 1c) or 5 μM chloroquine (column CQ).

In both cases, a 12 h application prevented the parasite development, and no hemozoin was seen in the food vacuole (Figure 8, **1c** 12 h, CQ 12 h). Prolonged incubation with compound **1c** led to parasite condensation and appearance of pycnotic forms (Figure 8, **1c** 25 h) contrasting with the shapeless, uncondensed forms observed with chloroquine (Figure 8, CQ 25 h). Thus, our results show that compound **1c** is inhibitory to trophozoite development and prevents the formation of hemozoin.

3. DISCUSSION

The role of redox enzymes in allowing the establishment of a microenvironment for parasite development is well-known. It is

clinically validated by the observation made in hemoglobinopathies that increasing the oxidative stress in erythrocytes confers a milieu hostile for parasite development. Prevalence of glucose-6-phosphate dehydrogenase (G6PDH) deficiency with 400 million people affected coincides with that of malaria with a very similar global distribution; this supports the so-called malaria protection hypothesis.[25] In particular, the parasites do not develop well in G6PDH-deficient red blood cells[26] or in erythrocytes depleted in GR activity[27] or in de novo biosynthesis of glutathione.[28] At the biochemical level, G6PDH is the first enzyme of the pentose phosphate pathway (hexose monophosphate shunt, HMS in Figure 1), which provides the reducing power of the cells in the form of NADPH. As NADPH is the only reducing substrate for GR in erythrocytes, G6PDH deficiency in red blood cells can be regarded as a natural knock-down version of human GR. G6PDH deficiency is not a serious condition for humans but prevents a severe malaria attack because the low antioxidative capacity in the red blood cells makes the milieu hostile for *Plasmodium*. Consequently, rapid elimination of parasitized G6PDH-deficient cells from the circulation occurs by enhanced phagocytosis via complement activation.[29] This important observation was recently supported by data from Arese and Becker's groups.[30] Human GR deficiency or drug-induced GR inhibition may protect from malaria via inducing enhanced ring stage phagocytosis by macrophages rather than by impairing parasite growth directly. Thus, mimicking G6PDH deficiency by GR redox-cyclers and other GR-targeting compounds represents a challenge to design new preclinical candidates as antimalarial drugs. However, these drugs must not trigger hemolysis both in G6PDH-sufficient and in G6PDH-deficient individuals.[31] This essential prerequisite could be reached using a prodrug approach or an enzyme-drug bioactivation process. The most relevant examples of this strategy are being exemplified by the first-discovered synthetic antimalarial drug, methylene blue (MB),[32] and, in the present work, by our lead antimalarial benzylNQ **1** (Figure 2).[33] These compounds lead to the killing of the malarial parasites, as reported here.

To develop this strategy, the synthesis and the screening of more than 100 new menadione derivatives for antimalarial activity allowed us to characterize a new series of potent antimalarial benzylNQ analogues **1** that are active both in vitro (in the low nanomolar range against the tested *P. falciparum* Dd2 strain) as well as in vivo. The selected compounds displayed no observable toxic effects against the human KB and MRC-5 cell lines or in mice. These lead benzylNQ are proposed to be metabolized to benzoylNQ through a cascade of redox reactions, involving a heme-catalyzed benzylic oxidation reaction under the specific conditions found in the acidic vesicles/food vacuole of the parasites, and then by a highly effective GR-catalyzed reduction in the cytosol. This last step was confirmed to be essential for the bioactivation of the benzylNQ series because GR inactivation by a potent suicide-substrate generated in the parasites led to the abolishment of the antimalarial activity of the parent difluorinated benzylNQ. From the mechanistic point of view, the benzoylNQ metabolites, in oxidized form (1,4-NQ core), were shown to act as the most efficient subversive substrates of reduced GR described so far and, in reduced form (hydro-1,4-NQ core), to convert metHb to Hb. The reduced species of benzoylNQ are assumed to be transported through Fe^{III} complexation into the food vacuole where the electrons are transferred to oxidants (heme and metHb). Subsequently, in oxidized forms, the benzoylNQ might be transported into the cytosol where they are reduced by the cytosolic GR (either from human erythrocyte or from the parasite) in a continuous redox cycle (Figure 2). This work provides a new strategy based on the particular situation of electrochemically active *P. falciparum*-infected erythrocytes in the presence of redox-cyclers, transported as charged species between two compartments, the anodic one for oxidation reactions (acidic vesicle/food vacuole network), and the cathodic one for reduction reactions (cytosol), possibly via iron complexation.[11d,34] Starting with *P. falciparum*-infected red blood cells and glucose as energy source, the benzoylNQ were designed to serve as membrane-permeable redox mediators and a source of electrons to inhibit the trophozoite development. Noteworthy is the fact that no harm is expected from human GR subversive substrates in all other host cells containing a nucleus because of the high flux control in these cells, for instance, by the de novo enzyme synthesis. Only host red blood cells, which have no nucleus and no possibility to regulate the glutathione biosynthesis, can be sensitive to reversible glutathione reductase inhibitors. This distinct situation between red blood cells and other nucleated cells represent the Achilles' heel on which we cash in as the cotarget of our drug design strategy.

A second reason to target the reduction of metHb is that the ferric form of hemoglobin is not capable of oxygen transport. A decreased oxygen carrying capacity of blood due to anemia is exacerbated by reduction in oxygen carrying capacity; this might proceed from even a modest concentration of metHb leading to an impaired supply of oxygen for the tissue. The reduction of metHb(Fe^{III}) to Hb(Fe^{II}) is of great importance in the treatment of malaria. High levels of metHb are observed in nonparasitized human red blood cells during *Plasmodium vivax* infections,[35a] during *Plasmodium yoelii nigeriensis* infection in mouse erythrocytes,[35b] and also in primaquine (PQ)- or dapsone-treated patients with G6PDH deficiency.[36,37] In the case of PQ, methemoglobinemia was recently shown to result from the transfer of one electron both from iron of Hb and the metabolite of PQ, 5-hydroxyPQ, to the π^* orbital of O_2.[38] This favors the formation of H_2O_2 and the accumulation of metHb. In the present work, a high benefit of our strategy originates from the fact that the expected metabolites generated from the lead benzylNQ are effective substrates of GR; thus, the product, the reduced benzoylNQ, redox-cycles metHb to Hb. This is not the case of PQ and other 8-aminoquinolines. Nevertheless, optimizing and developing our lead benzylNQ into preclinical candidates will involve several challenges concerning the pathophysiology of hemolysis in G6PDH patients. As there is no pharmacologically validated model today for hemolysis in G6PDH-deficient populations, we are setting up such a platform to determine and to predict any detrimental effects on G6PDH-deficient red blood cells from patients at risk.

In summary, the antimalarial 1,4-naphthoquinones are proposed to act catalytically as redox-active biosensors that are cycled in and out the food vacuole in infected red blood cells, thereby oxidizing major intracellular reductants (like NADPH in the cytosol) and subsequently reducing the oxidants (hematin and metHb). Ultimately, the antimalarial 1,4-naphthoquinones are suggested to affect the redox equilibrium in the parasites, drowning the parasite in its own metabolic products. They will serve as lead compounds for further structural refinement with improved solubility and/or bioavailability.

In the long term, the results from our interdisciplinary approach will provide detailed insight into the understanding of how redox-cyclers interfere with the putative negative cooperativity of GR toward NADPH binding and how this property can be exploited for disulfide reductase-catalyzed drug

bioactivation as a general concept to open a new perspective in medicinal chemistry. The mechanism of this putative negative cooperativity toward NADPH binding remains to be proved and orientates the future direction of our investigations.

4. EXPERIMENTAL SECTION

4.1. Chemistry. Melting points were determined on a Büchi melting point apparatus and were not corrected. ^{1}H (300 MHz) and ^{13}C (75 MHz) NMR spectra were recorded on a Bruker DRX-300 spectrometer; chemical shifts were expressed in ppm relative to tetramethylsilane (TMS); multiplicity is indicated as s (singlet), d (doublet), t (triplet), q (quartet), sep (septet), m (multiplet), cm (centered multiplet), dd (doublet of a doublet), dt (doublet of a triplet), and td (triplet of a doublet). C_q indicates a quaternary carbon in the ^{13}C NMR assignation. ^{19}F NMR was performed using 1,2-difluorobenzene as external standard (δ = −139.0 ppm). Intensities in the IR spectra are indicated as vs (very strong), s (strong), m (medium), w (weak), and b (broad). Elemental analyses were carried out at the Mikroanalytisches Laboratorium der Chemischen Fakultät der Universität Heidelberg. Electron impact mass spectrometry (EI MS) and chemical ionization mass spectrometry (CI MS), were recorded at facilities of the Institut für Organische Chemie der Universität Heidelberg. Analytical TLC was carried out on precoated Sil G-25 UV_{254} plates from Macherey&Nagel. Flash chromatography was performed using silica gel G60 (230−400 mesh) from Macherey&Nagel.

General Procedure for the Silver-Catalyzed Radical Decarboxylation Reactions of 1,4-Naphthoquinones with Carboxylic Acids. A solution of menadione or plumbagin (5.81 mmol) and of phenylacetic acid derivative (11.58 mmol) in 52.5 mL of acetonitrile and 17.5 mL of water was heated to 85 °C. $AgNO_3$ (90 mg, 0.58 mmol) was added. $(NH_4)_2S_2O_8$ (1.72 g, 7.54 mmol) in 15 mL of acetonitrile and 5 mL of water was added dropwise over a period of 45 min and then heated at reflux for 2 h. The acetonitrile was removed in vacuo. The aqueous phase was extracted with dichloromethane (4 × 10 mL), dried over $MgSO_4$, and purified by flash chromatography.

*2-(4-Bromobenzyl)-3-methylnaphthalene-1,4-dione (**1a**).* As starting materials for the radical decarboxylation reaction, menadione and 4-bromophenylacetic acid were used. After chromatography on silica gel (PE:CH_2Cl_2 = 1:1, UV), 3.10 g (9.12 mmol, 78% yield) of **1a** was isolated as a yellow solid. mp 121−122 °C. ^{1}H NMR (300 MHz, $CDCl_3$): δ 8.03−8.10 (m, 2H), 7.66−7.71 (m, 2H), 7.36 (dt, ^3J = 8.46 Hz, ^4J = 1.95 Hz, 2H), 7.09 (d, ^3J = 8.53 Hz, 2H), 3.96 (s, 2H), 2.22 (s, 3H). ^{13}C NMR (75 MHz, $CDCl_3$): δ 185.20 (C_q), 184.54 (C_q), 144.75 (C_q), 144.57 (C_q), 137.06 (C_q), 133.58 (CH), 132.08 (C_q), 131.94 (C_q), 131.71 (CH), 130.32 (CH), 126.50 (CH), 126.35 (CH), 120.31 (C_q), 31.93 (CH_2), 13.31 (CH_3). IR (KBr): ν = 3449 (b, w), 3068 (w), 2962 (w), 1661 (vs), 1624 (m), 1618 (m), 1594 (s), 1486 (s), 1376 (m), 1332 (s), 1315 (s), 1294 (vs), 1071 (m), 1010 (s), 971 (w), 815 (m), 787 (s), 730 (m), 702 (m), 629 (w), 426 cm^{-1} (w). EI MS (70 eV, m/z (%)): 340.1 ([M]$^+$, 13), 325.0 (100), 246.1 (63), 215.1 (41), 202.1 (49), 128.1 (72), 76.0 (74). Anal. Calcd for $C_{18}H_{13}BrO_2$: C, 63.36; H, 3.84. Found: C, 63.02; H, 3.84.

*2-(4-Bromobenzyl)-3-(difluoromethyl)naphthalene-1,4-dione (**7a**).* As starting materials for the radical decarboxylation reaction, difluoromenadione and 4-bromophenylacetic acid were used. After chromatography on silica gel (PE:CH_2Cl_2 = 1:1, UV), 132 mg (0.35 mmol, 73% yield) of **7a** was isolated as a yellow solid. mp 103−104 °C. ^{1}H NMR (300 MHz, $CDCl_3$): δ 8.07−8.13 (m, 1H), 7.99−8.05 (m, 1H), 7.70−7.79 (m, 2H), 7.36 (d, ^3J = 8.46 Hz, 2H), 7.24 (t, ^1J = 53.87 Hz, 1H, CHF_2), 7.18 (d, ^3J = 8.42 Hz, 2H), 4.19 (s, 2H). ^{13}C NMR (75 MHz, $CDCl_3$): δ 184.38 (C_q), 182.79 (C_q), 149.21 (C_q), 136.03 (C_q), 134.41 (CH), 131.76 (C_q), 131.63 (CH), 130.89 (CH), 126.87 (CH), 126.54 (CH), 120.67 (C_q), 110.45 (CHF_2, ^1J = 239.85 Hz), 31.66 (CH_2). IR (KBr): ν = 3436 (b, w), 3100 (w), 3076 (w), 3049 (w), 3018 (w), 2936 (w), 1672 (vs), 1657 (vs), 1625 (s), 1594 (s), 1487 (vs), 1406 (m), 1329 (s), 1297 (vs), 1181 (m), 1123 (s), 1082 (s), 1071 (m), 1035 (vs), 1013 (s), 876 (m), 831 (s), 788 (s), 733 (s), 713 (m), 535 cm^{-1} (m). EI MS (70 eV, m/z (%)): 377.1 ([M]$^+$, 21), 325.1 (11), 257.1 (10), 169.0 (100), 90.1 (18). Anal. Calcd for $C_{18}H_{11}BrF_2O_2$: C, 57.32; H, 2.94. Found: C, 57.01; H, 3.12.

General Procedure for the Oxidation of Benzyl Derivatives to the Corresponding Benzoyl Derivatives. H_5IO_6 (1.40 g, 6.16 mmol) was dissolved in 25 mL of acetonitrile by vigorous stirring, and then CrO_3 (17.6 mg, 0.18 mmol) was dissolved into the mixture to give an orange solution. The benzyl-derivative (0.88 mmol) was added to the above solution with stirring. The solution turned to an orange suspension within a few seconds that turned yellow after a few minutes. The solution was stirred at room temperature until all starting material was consumed (TLC control). The solvent was removed in vacuo, and the residue was purified by flash chromatography to give the corresponding benzoyl-derivative.

*2-(4-Bromobenzoyl)-3-methylnaphthalene-1,4-dione (**3a**).* As starting material, **1a** was used. After chromatography on silica gel (PE:CH_2Cl_2 = 1:3, UV), 133 mg (0.38 mmol, 43% yield) of **3a** was isolated as a yellow solid. mp 170−171 °C. ^{1}H NMR (300 MHz, $CDCl_3$): δ 8.14−8.17 (m, 1H), 8.03−8.06 (m, 1H), 7.73−7.81 (m, 4H), 7.64 (t, ^3J = 2.08 Hz, 1H), 7.61 (t, ^3J = 1.95 Hz, 1H), 2.05 (s, CH_3). ^{13}C NMR (75 MHz, $CDCl_3$): δ 192.72 (C_q), 184.63 (C_q), 183.32 (C_q), 144.30 (C_q), 143.85 (C_q), 134.49 (C_q), 134.30 (CH), 134.19 (CH), 132.48 (CH), 131.87 (C_q), 131.49 (C_q), 130.52 (CH), 130.01 (C_q), 126.78 (CH), 126.44 (CH), 13.60 (CH_3). IR (KBr): ν = 3442 (b, m), 1669 (vs), 1653 (vs), 1627 (vs), 1586 (m), 1568 (m), 1398 (m), 1378 (m), 1329 (s), 1291 (vs), 1272 (s), 1241 (m), 1176 (m), 1069 (m), 1011 (m), 978 (s), 864 (m), 784 (s), 722 (m), 692 cm^{-1} (m). EI MS (70 eV, m/z (%)): 353.9 ([M]$^+$, 41), 275.0 (100), 182.9 (71), 115.0 (50), 76.0 (41). Anal. Calcd for $C_{18}H_{11}BrO_3$: C, 60.87; H, 3.12; Br, 22.50. Found: C, 60.96; H, 3.24; Br, 22.60.

*2-(4-Bromobenzoyl)-3-(difluoromethyl)-naphthalene-1,4-dione (**8a**).* As starting material, **7a** was used. 40 mg (0.10 mmol, 78% yield) of **8a** was isolated as a yellow solid. mp = 135−137 °C. ^{1}H NMR (300 MHz, $CDCl_3$): δ 8.20 (dd, 1H, ^3J = 7,1 Hz, ^4J = 1,9 Hz), 8.10 (dd, 1H, ^3J = 7,2 Hz, ^4J = 1,8 Hz), 7.84−7.89 (m, 2H), 7.75 (d, 2H, ^3J = 8,6 Hz), 7.65 (d, 2H, ^3J = 8,6 Hz), 6.90 (t, 1H, ^2J = 53,3 Hz). ^{13}C NMR (75 MHz, $CDCl_3$): δ 189.86 (C_q), 183.38 (C_q), 182.44 (C_q), 144.38 (C_q), 135.30 (C_q), 135.28 (CH), 135.18 (CH), 134.34 (C_q), 132.35 (CH), 131.91 (CH), 131.67 (CH), 130.91 (C_q), 130.42 (CH), 130.04 (C_q), 126.91 (CH), 126.87 (CH), 125.70 (C_q), 110.02 (CHF_2). EI MS (70 eV, m/z (%)): 391.9 ([M]$^+$, 26), 326.9 (35), 200.0 (40), 182.9 (100), 154.9 (30), 104.0 (26), 76.1 (25). Anal. Calcd for $C_{18}H_9BrF_2O_3$: C, 55.27; H, 2.32. Found: C, 54.92; H, 2.85.

*2-(Difluoromethyl)-1,4-dimethoxynaphthalene **19**.* The reaction was conducted in a Teflon bottle under N_2-atmosphere. To a solution of 750 mg (3.47 mmol) of 1,4-dimethoxy-naphthalene-2-carbaldehyde in 10 mL of dry CH_2Cl_2 were added 775 μL (950 mg, 5.90 mmol) DAST and 10 μL (0.17 mmol) ethanol at 0 °C. The reaction mixture was stirred for 1 h at this temperature and then heated overnight to 40 °C. To run the reaction to completion, another 140 μL of DAST was added followed by incubation at 40 °C for additional 5 h. Ten milliliters of saturated $NaHCO_3$ solution was added in small portions to quench the reaction. The organic phase was separated, and the aqueous phase was extracted with CH_2Cl_2 (2 × 20 mL), dried over $MgSO_4$, and purified by flash-chromatography on silica gel (PE:CH_2Cl_2 = 1:1, UV) to give 723 mg of **19** (3.03 mmol, 88%) of an almost colorless solid. mp 44−46 °C. ^{1}H NMR (300 MHz, $CDCl_3$): δ 8.25−8.30 (m, 1H), 8.06−8.11 (m, 1H), 7.53- 7.62 (m, 2H), 7.16 (t, ^1J = 55.8 Hz, 1H, CHF_2), 6.90 (s, 1H), 4.02 (s, 3H), 3.97 (s, 3H). ^{13}C NMR (75 MHz, $CDCl_3$): δ 152.3 (C_q), 148.5 (C_q), 127.9 (C_q), 126.9 (CH), 126.7 (CH), 122.6 (C_q), 122.5 (CH), 122.2 (C_q), 122.0 (CH), 111.7 (t, ^1J = 235 Hz, CHF_2), 98.6

(CH), 63.8 (CH_3), 55.5 (CH_3). ^{19}F NMR ($CDCl_3$): δ −112.37 (d, ^1J = 55.8 Hz). EI MS (70 eV, m/z (%)): 238.07 ([M]$^+$, 95), 223.0 (100). Anal. Calcd for $C_{13}H_{12}F_2O_2$: C, 65.54; H, 5.08. Found: C, 65.39; H, 5.20.

2-(Difluoromethyl)naphthalene-1,4-dione (or Difluoromenadione). 500 mg (2.10 mmol) of 2-difluoromethyl-1,4-dimethoxy-naphthalene **19** was dissolved in 10 mL of CH_3CN, and a solution of 3.45 g (6.30 mmol) of CAN in 8 mL of H_2O was added. The reaction mixture was stirred for 15 min at room temperature, the acetonitrile was removed in vacuo, and the product was extracted with CH_2Cl_2 (5 × 10 mL), dried over $MgSO_4$, and purified by flash-chromatography on silica gel (PE:CH_2Cl_2 = 1:1, UV) to give 405 mg of difluoromenadione as a yellow solid (1.95 mmol, 93%). mp 74 °C. ^{1}H NMR (300 MHz, $CDCl_3$): δ 8.07−8.15 (m, 2H), 7.76−7.83 (m, 2H), 7.19 (m, 1H), 6.83 (t, ^1J = 53.9 Hz, C*H*F$_2$, 1H). ^{13}C NMR (75 MHz, $CDCl_3$): δ 183.9 (C_q), 182.4 (C_q), 140.4 (t, ^2J = 21.2 Hz, C_q), 135.1 (CH), 134.9 (CH), 134.3 (CH), 134.2 (CH), 131.6 (C_q), 131.3 (C_q), 126.4 (CH), 109.2 (t, ^1J = 240.4 Hz, CHF_2). ^{19}F NMR ($CDCl_3$): δ −123.85 (d, ^1J = 53.9 Hz). EI MS (70 eV, m/z (%)) 208.02 ([M$^+$], 100) calcd 208.03. Anal. Calcd for $C_{11}H_6F_2O_2$: C, 63.47; H, 2.91. Found: C, 63.58; H, 3.02.

4.2. In Vitro Antiparasitic Bioassays. *P. falciparum* in vitro culture was carried out using standard protocols[39] with modifications.[12b] Drug susceptibility of *P. falciparum* was studied using a modified method[18] of the protocol described previously for the ^{3}H-hypoxanthine incorporation-based assay.[19] All assays included CQ diphosphate (Sigma, UK) as standard and control wells with untreated infected and uninfected erythrocytes. IC_{50} values were derived by sigmoidal regression analysis (Microsoft *xl*fit).

Determination of IC_{50} Values against Dd2 P. falciparum Strain. The IC_{50} was tested by standard in vitro antiproliferation assays based on the ^{3}H-hypoxanthine incorporation.[19] Infected erythrocytes in ring stage (0.5% parasitemia, 2.5% hematocrit) in 96-well plates were exposed to the compounds for 48 h and then to radioactive hypoxanthine for 24 h. The amount of radioactivity in precipitable material served as an index of cell proliferation. Chloroquine was added as reference and displayed an IC_{50} value of 110 nM.

4.3. Enzymes. Recombinant human and *Plasmodium falciparum* glutathione reductases were purified as previously reported.[32a,40] One unit of GR activity is defined as the consumption of 1 μmol of NADPH per min $\varepsilon_{340\ nm}$ = 6.22 mM^{-1} cm^{-1}) under conditions of substrate saturation. The enzyme stock solutions used for kinetic determinations were >98% pure as judged from silver stained SDS-PAGE and had specific activities of 200 U/mg (human GR) and 120 U/mg (*P. falciparum* GR). All other reagents were of the highest available purity and were purchased from Biomol, Boehringer, and Sigma.

Glutathione Disulfide Reduction Assays. The standard assay was conducted at 25 °C in a 1 mL cuvette. The assay mixture contained 100 μM NADPH and 1 mM GSSG in GR buffer (100 mM potassium phosphate buffer, 200 mM KCl, 1 mM EDTA, pH 6.9). IC_{50} values were evaluated in duplicate in the presence of seven inhibitor concentrations ranging from 0 to 100 μM. Inhibitor stock solutions were prepared in 100% DMSO. 1% DMSO concentration was kept constant in the assay cuvette. The reaction was started by adding enzyme (8 mU human GR, 6.5 mU *P. falciparum* GR), and initial rates of NADPH oxidation were monitored at 340 nm ($\varepsilon_{340\ nm}$ = 6.22 mM^{-1} cm^{-1}). Inhibition of GSSG reduction by **3f** was measured as a function of substrate concentration, and the data were fitted by using a nonlinear regression analysis software (Kaleidagraph) to the equation for uncompetitive inhibition.[11a]

1,4-Naphthoquinone Reductase Activity of P. falciparum Glutathione Reductase. The reduction assay mixture consisted of 100 mM potassium phosphate buffer pH 6.9, 200 mM KCl, 1 mM EDTA, and 100 μM NADPH in a total volume of 1 mL. 1,4-Naphthoquinone reductase activity was determined by recording the initial velocities in the presence of increasing naphthoquinone concentrations (0−300 μM). The 1,4-naphthoquinone was first dissolved in DMSO, and a final 1% DMSO concentration was kept constant in the 1,4-naphthoquinone reductase assay. For the determination of K_m and V_{max} values, the steady-state rates were fitted by using nonlinear regression analysis software (Kaleidagraph) to the Michaelis−Menten equation. From these values, the turnover number k_{cat} and the catalytic efficiency k_{cat}/K_m were calculated.

4.4. Time-Dependent Inactivation of Glutathione Reductases by Difluoromenadione, 7a and 8a. For determining the rate constants of human GR inactivation, the residual GR activity was monitored over time by following an incubation protocol. All reaction mixtures (final volume of 50 μL) contained 160 μM NADPH, varying inhibitor concentrations (0−5 μM in the human GR assay; 0−50 μM in the *P. falciparum* GR assay), GR (6.85 pmol of human GR; 21 pmol of *P. falciparum* GR), 2% DMSO in GR buffer at 25 °C. At different time points (<10 min), 5 μL aliquots of each reaction mixture were removed, and the residual activity was measured in the standard GSSG reduction assay at 25 °C (1 mM GSSG and 100 μM NADPH). 2% DMSO was used in control assays.

4.5. Methemoglobin Reduction in the Presence of BenzoylNQ 3a or 3d or MB upon Reduction by the NADPH−GR System. In an Eppendorf tube containing 6.4 mg of human metHb dissolved in 885 μL of GR buffer (47 mM potassium phosphate buffer pH 6.9, 200 mM KCl, 100 mM EDTA), 10 μL of 20 mM **3a** dissolved in DMSO and 100 μL of NADPH dissolved in GR buffer were added. The reaction was started by the addition of 5 μL of human GR (1.06 μmol) and then incubated at 37 °C. In a 1 mL cuvette, 20 μL of the reaction mixture was diluted with 980 μL of GR buffer. UV−vis spectral absorption changes induced by the benzoylNQ **3d**, or the controls MB or CQ, on methemoglobin chromophore were monitored from 300 to 700 nm on a Cary 50 (Varian) spectrophotometer maintained at 37 °C after 0, 5, 10, 20, and 30 min incubation time. The final concentrations in the reaction mixture were 100 μM metHb, 200 μM benzoylNQ or MB, 400 μM NADPH, and 1.06 μmol hGR, final DMSO concentration 1%, 37 °C. No metHb reduction was observed in the presence of CQ, which was used as negative control.

*Direct Methemoglobin Reduction in the Presence of the 3-Benzoyldihydronaphthoquinone **20**.* The UV−vis spectral absorption changes induced by 40 μM dihydronaphthoquinone **20** on 2 μM methemoglobin chromophore were directly monitored in the cuvette from 250 to 550 nm on a Cary 300 (Varian) spectrophotometer maintained at 37.5 °C by the flow of a Lauda E200 thermostat. The Scanning Kinetics application in FLWinLab software was used to monitor the spectral changes versus time with the following instrumental parameters: spectral window, 250−550 nm; number of cycles, 30; cycle time, 45 s; scanning rate, 200 nm/min; interval, 1 nm.

4.6. Evaluation of Cytotoxicity of the Different Drugs against Human Cell Lines. *Evaluation of the Cytotoxicity against Human KB Cells.* Cytotoxicity on human KB cells (human oral pharyngeal carcinoma) was evaluated using the resazurin (Alamar Blue) assay as described.[18] The positive control drug was podophyllotoxin (Sigma). IC_{50} values were calculated as compared to blanks and untreated controls.

Evaluation of the Cytotoxicity against Human MRC-5 Cells. Human MRC-5$_{SV2}$ cells are cultured in Earl's MEM + 5% FCSi. Assays are performed in 96-well microtiter plates, each well containing about 10^4 cell/well. After 3 days incubation, cell viability is assessed fluorimetrically after addition of resazurin and fluorescence is measured (λ_{ex} 550 nm, λ_{em} 590 nm).[18] The results are expressed as % reduction in cell growth/viability as compared to untreated control wells and IC_{50} is determined. Compounds are tested at five concentrations (64−14− 4−1−0.25 μM or mg/mL). When the IC_{50} is lower than 4 μg/mL or μM, the compound is classified as toxic.

4.7. Determination of % Parasitemia in CD1Mice. The in vivo tests in the mouse model were done according to a standard

protocol.[41] Compounds were tested in the ANKA *P. berghei* model by using the 4-day suppressive test, as indicated by Peters, and using chloroquine as a positive control. Briefly, naive 18−20 g CD1 mice were infected intravenously with 2×10^6 parasitized red cells on day +0. For administration, compounds were freshly prepared in 10% DMSO in sterile phosphate-buffered saline the day of use. Two hours postinfection, mice received the first treatment by the intraperitoneal route. Mice were further treated on days +1−3. Blood films from tail blood were prepared on day +4, and parasitemia was determined by microscopic examination of Giemsa-stained blood films. Compounds were tested with a daily dose of 50 or 30 mg/kg by the intraperitoneal or oral route. Chloroquine treatment p.o. at 10 mg/kg/day was included as a positive control and resulted in complete inhibition (data not shown). Intraperitoneous administrations of CQ have shown similar activity (98.9% inhibition at 10 mg/kg i.p). Mice were treated, and levels of parasitemia were determined as described.

4.8. Morphological Examination of *P. falciparum* Trophozoite Development Inhibition by Compound 1c. The FcB1 strain of *P. falciparum* was routinely grown in human erythrocytes and RPMI medium supplemented with 8% heat-inactivated human plasma under a 91% N_2, 6% O_2, and 3% CO_2 atmosphere. Parasites were synchronized on a 0−5 h time window by successive Plasmion[42] and sorbitol[43] treatments. Dose−response assay based upon [^{3}H]-hypoxanthine incorporation by growing parasites[19] was used to determine the inhibitory concentrations of compound **1c**. Shortly, 16−21 h-old parasites (trophozoites) were incubated for 48 h in the presence of decreasing concentrations of compound **1c** and 0.25 μCi [^{3}H]-hypoxanthine. IC_{50} and $IC_{100\ min}$ values were determined from the resulting dose−response curves; they correspond to the drug concentration required to observe 50% and 100% of the inhibition of the parasitic growth, respectively (min means minimal drug concentration). For analysis of compound **1c**-induced morphological alterations, trophozoites (16−21 h-old) were grown for 25 h at 1% parasitemia and 2% hematocrit in culture medium supplemented with 5 μM ($IC_{100\ min}$) compound **1** or 5 μM chloroquine. Control for normal growth was in culture medium alone. Diff Quick-stained smears were made every 2 h during 12 h and then after 25 h, and were analyzed by optical examination.

■ ASSOCIATED CONTENT

Supporting Information. Detailed experimental procedures, spectroscopic data, and elemental analyses for the preparation and the characterization of the new compounds **1**−**20**, and cytotoxicity activities against human cells. This material is available free of charge via the Internet at http://pubs.acs.org.

■ AUTHOR INFORMATION

Corresponding Author
elisabeth.davioud@unistra.fr

Author Contributions
#These authors contributed equally.

■ ACKNOWLEDGMENT

E.D.-C. is a delegate of Centre National de la Recherche Scientifique, in the frame of a French−German cooperation with Heidelberg University, Germany. E.D.-C. thanks DFG via the SFB 544 (B14 project) and CNRS for financial support. R.H.S. and M.L. thank DFG via the SFB 544 (B2 and B12 projects). T.M. thanks Prof. Thomas J. J. Müller for fruitful discussions during the P.h.D thesis work. We are grateful to Dr. Mourad Elhabiri, Strasbourg University, for the direct metHb reduction experiment, Dr. Hervé Vezin for the residual data of cyclic voltammetry carried out in the experiments previously reported,[11b] and Prof. Louis Maes, Antwerp University, for the primary cytotoxicity assays with the human MRC-5 cell line.

■ REFERENCES

(1) White, N. J. *Lancet* **2010**, *376*, 2051–2052.
(2) Zarchin, S.; Krugliak, M.; Ginsburg, H. *Biochem. Pharmacol.* **1986**, *35*, 2435–2442.
(3) (a) Abu-Bakar, N.; Klonis, N.; Hanssen, E.; Chan, C.; Tilley, L. *J. Cell Sci.* **2010**, *123*, 441–450. (b) Ncokazi, K. K.; Egan, T. J. *Anal. Biochem.* **2005**, *338*, 306–319. (c) Cohen, S. N.; Phifer, K. O.; Yielding, K. L. *Nature* **1964**, *202*, 805–806. (d) Egan, T. J. *J. Inorg. Biochem.* **2006**, *100*, 916–926. (e) Egan, T. J. *J. Inorg. Biochem.* **2008**, *102*, 1288–1299.
(4) Dorn, A.; Stoffel, R.; Matile, H.; Bubendorf, A.; Ridley, R. *Nature* **1995**, *374*, 269–271.
(5) Loria, P.; Miller, S.; Foley, M.; Tilley, L. *Biochem. J.* **1999**, *339*, 363–370.
(6) (a) Atamna, H.; Ginsburg, H. *J. Biol. Chem.* **1995**, *270*, 24876–83. (b) Ginsburg, H.; Famin, O.; Zhang, J.; Krugliak, M. *Biochem. Pharmacol.* **1998**, *56*, 1305–1313.
(7) Vippagunta, S. R.; Dorn, A.; Ridley, R. G.; Vennerstrom, J. L. *Biomed. Biochim. Acta* **2000**, *1475*, 133–140.
(8) Hogg, T.; Nagarajan, K.; Herzberg, S.; Chen, L.; Shen, X.; Jiang, H.; Wecke, M.; Blohmke, C.; Hilgenfeld, R.; Schmidt, C. L. *J. Biol. Chem.* **2006**, *281*, 25425–25437.
(9) Monti, D.; Vodopivec, B.; Basilico, N.; Olliaro, P.; Taramelli, D. *Biochemistry* **1999**, *38*, 8858–8863.
(10) (a) Schirmer, R. H.; Mueller, J. G.; Joachim, G.; Krauth-Siegel, R. L. *Angew. Chem., Int. Ed. Engl.* **1995**, *34*, 141–154. (b) Krauth-Siegel, R. L.; Bauer, H.; Schirmer, R. H. *Angew. Chem., Int. Ed.* **2005**, *44*, 690–715.
(11) (a) Biot, C.; Bauer, H.; Schirmer, R. H.; Davioud-Charvet, E. *J. Med. Chem.* **2004**, *47*, 5972–5983. (b) Bauer, H.; Fritz-Wolf, K.; Winzer, A.; Kühner, S.; Little, S.; Yardley, V.; Vezin, H.; Palfey, B.; Schirmer, R. H.; Davioud-Charvet, E. *J. Am. Chem. Soc.* **2006**, *128*, 10784–10794. (c) Morin, C.; Besset, T.; Moutet, J.-C.; Fayolle, M.; Brückner, M.; Limosin, D.; Becker, K.; Davioud-Charvet, E. *Org. Biomol. Chem.* **2008**, *6*, 2731–2742.(d) Davioud-Charvet, E.; Lanfranchi, D. A. In *Apicomplexan Parasites − Molecular Approaches toward Targeted Drug Development*; Becker, K., Selzer, P. M., Eds.; Wiley-VCH: Weinheim, 2011; Vol. 2 (Drug Discovery in Infectious Diseases).
(12) (a) Davioud-Charvet, E.; Delarue, S.; Biot, C.; Schwöbel, B.; Böhme, C. C.; Müssigbrodt, A.; Maes, L.; Sergheraert, C.; Grellier, P.; Schirmer, R. H.; Becker, K. *J. Med. Chem.* **2001**, *44*, 4268–4276. (b) Friebolin, W.; Jannack, B.; Wenzel, N.; Furrer, J.; Oeser, T.; Sanchez, C. P.; Lanzer, M.; Yardley, V.; Becker, K.; Davioud-Charvet, E. *J. Med. Chem.* **2008**, *51*, 1260–1277.
(13) (a) Subba-Rao, R. V.; Alexander, M. *Appl. Environ. Microbiol.* **1985**, *49*, 509–516. (b) Segrestaa, J.; Verite, P.; Estour, F.; Menager, S.; Lafont, O. *Chem. Pharm. Bull.* **2002**, *50*, 744–748.
(14) (a) Jaffé, E. R.; Neurmann, G. *Nature* **1964**, *202*, 607–608. (b) Beutler, E.; Baluda, M. C. *Blood* **1963**, *22*, 323–233.
(15) Kochi, J. K.; Anderson, J. M. *J. Am. Chem. Soc.* **1970**, *92*, 1651–1659.
(16) Yamazaki, S. *Org. Lett.* **1999**, *1*, 2129–2132.
(17) Evans, P. A.; Brandt, T. A. *J. Org. Chem.* **1997**, *62*, 5321–5326.
(18) O'Brien, J.; Wilson, I.; Orton, T.; Pognan, F. *Eur. J. Biochem.* **2000**, *267*, 5421–5426.
(19) Desjardins, R. E.; Canfield, C. J.; Haynes, J. D.; Chulay, J. D. *Antimicrob. Agents Chemother.* **1979**, *16*, 710–718.
(20) (a) Hanoulle, X.; Wieruszeski, J. M.; Rousselot-Pailley, P.; Landrieu, I.; Locht, C.; Lippens, G.; Baulard, A. R. *J. Antimicrob. Chemother.* **2006**, *58*, 768–772. (b) Hanoulle, X.; Wieruszeski, J. M.; Rousselot-Pailley, P.; Landrieu, I.; Baulard, A. R.; Lippens, G. *Biochem. Biophys. Res. Commun.* **2005**, *331*, 452–458.

(21) Hünig, S.; Bau, R.; Kemmer, M.; Meixner, H.; Metzenthin, T.; Peters, K.; Sinzger, K.; Gulbis, J. *Eur. J. Org. Chem.* **1998**, 335–348.
(22) Kitz, R.; Wilson, I. B. *J. Biol. Chem.* **1962**, *237*, 3245–3249.
(23) Gulino, D.; Pham, Q. T.; Golé, J.; Pascault, J. P. *Anionic Polymerization*; ACS Symposium Series; American Chemical Society: Washington, DC, 1981; Vol. 166, Chapter 20, pp 307−326.
(24) Jain, M.; Vangapandu, S.; Sachdeva, S.; Singh, S.; Singh, P. P.; Jena, G. B.; Tikoo, K.; Ramarao, P.; Kaul, C. L.; Jain, R. *J. Med. Chem.* **2004**, *47*, 285–287.
(25) Cappellini, M. D.; Fiorelli, G. *Lancet* **2008**, *371*, 64–74.
(26) Ginsburg, H.; Atamna, H.; Shalmiev, G.; Kanaani, J.; Krugliak, M. *Parasitology* **1996**, *113*, 7–18.
(27) (a) Zhang, Y. A.; Hempelmann, E.; Schirmer, R. H. *Biochem. Pharmacol.* **1988**, *37*, 855–860. (b) Zhang, Y.; König, I.; Schirmer, R. H. *Biochem. Pharmacol.* **1988**, *37*, 861–865.
(28) Lüersen, K.; Walter, R. D.; Müller, S. *Biochem. J.* **2000**, *346*, 545–552.
(29) Cappadoro, M.; Giribaldi, G.; O'Brien, E.; Turrini, F.; Mannu, F.; Ulliers, D.; Simula, G.; Luzzatto, L.; Arese, P. *Blood* **1998**, *92*, 2527–2534.
(30) Gallo, V.; Schwarzer, E.; Rahlfs, S.; Schirmer, R. H.; van Zwieten, R.; Roos, D.; Arese, P.; Becker, K. *PLoS One* **2009**, *4*, e7303.
(31) Baird, J. K.; Surjadjaja, C. *Trends Parasitol.* **2011**, *27*, 11–16.
(32) (a) Färber, P. M.; Arscott, L. D.; Williams, C. H., Jr.; Becker, K.; Schirmer, R. H. *FEBS Lett.* **1998**, *422*, 311–314.(b) Schirmer, M.; Scheiwein, M.; Gromer, S.; Becker, K.; Schirmer, R. H. In *Flavins and Flavoproteins*; Ghisla, S., Kroneck, P., Macheroux, P., Sund, H., Eds.; Rudolf Weber, Agency for Scientific Publications: Berlin, 1999; pp 857−862. (c) Kasozi, D.; Gromer, S.; Adler, H.; Zocher, K.; Rahlfs, S.; Wittlin, S.; Fritz-Wolf, K.; Schirmer, R. H.; Becker, K. *Redox Rep.* **2011**, in press.
(33) Davioud-Charvet, E.; Müller, T.; Bauer, H.; Schirmer, R. H. Patent EP 08290278.4 (March 26, 2008); patent PCT/EP2009/053483 (March 25, 2009).
(34) Cohen, M. S.; Chai, Y.; Britigan, B. E.; McKenna, W.; Adams, J.; Svendsen, T.; Bean, K.; Hassett, D. J.; Sparling, P. F. *Antimicrob. Agents Chemother.* **1987**, *31*, 1507–1513.
(35) (a) Anstey, N. M.; Hassanali, M. Y.; Mlalasi, J.; Manyenga, D.; Mwaikambo, E. D. *Trans. R. Soc. Trop. Med. Hyg.* **1996**, *90*, 147–151. (b) Srivastava, S.; Alhomida, A. S.; Siddiqi, N. J. *In Vivo* **2000**, *14*, 547–550.
(36) Brabin, B. J.; Eggelte, T. A.; Parise, M.; Verhoeff, F. *Drug Saf.* **2004**, *27*, 633–48.
(37) Vale, N.; Moreira, R.; Gomes, P. *Eur. J. Med. Chem.* **2009**, *44*, 937–953.
(38) Liu, H.; Walker, L. A.; Nanayakkara, N. P.; Doerksen, R. J. *J. Am. Chem. Soc.* **2011**, *133*, 1172–75.
(39) Trager, W.; Jensen, J. B. *Science* **1976**, *193*, 673–675.
(40) Nordhoff, A.; Bucheler, U. S.; Werner, D.; Schirmer, R. H. *Biochemistry* **1993**, *32*, 4060–4066.
(41) Peters, W.; Robinson, B. L. *Handbook of Animal Models of Infection*; Academic Press: London, 1999; pp 756−771.
(42) Pasvol, G.; Wilson, R. J.; Smalley, M. E.; Brown, J. *Ann. Trop. Med. Parasitol.* **1978**, *72*, 87–88.
(43) Lambros, C.; Vanderberg, J. P. *J. Parasitol.* **1979**, *65*, 418–420.